

Adaptive Methods for Multiobjective Unit Commitment

Ece Tevruez and Aswin Kannan*

January 14, 2025

Abstract

This work considers a multiobjective version of the unit commitment problem that deals with finding the optimal generation schedule of a firm, over a period of time and a given electrical network. With growing importance of environmental impact, some objectives of interest include CO₂ emission levels and renewable energy penetration, in addition to the standard generation costs. Some typical constraints include limits on generation levels and up/down times on generation units. This further entails solving a multiobjective mixed integer optimization problem. The related literature has predominantly focused on heuristics (like Genetic Algorithms) for solving larger problem instances. Our major intent in this work is to propose scalable versions of mathematical optimization based approaches that help in speeding up the process of estimating the underlying Pareto frontier. Our contributions are computational and rest on two key embodiments. First, we use the notion of both epsilon constraints and adaptive weights to solve a sequence of single objective optimization problems. Second, to ease the computational burden, we propose a McCormick-type relaxation for quadratic type constraints that arise due to the resulting formulation types. We test the proposed computational framework on real network data from [1, 51] and compare the same with standard solvers like Gurobi. Results show a significant reduction in complexity (computational time) when deploying the proposed framework.

1 Introduction

The standard unit commitment problem [8, 15], also known as the OPF (Optimal Power Flow problem) considers the power planning problem of an agent with multiple generators housed in an electrical network. Besides cost minimization, this further requires meeting constraints on consumer demand, ramping, switching decisions of generators, the respective up-and-down times [17, 49], and network transmission levels. Up and downtime constraints are common in settings with conventional generators that use coal like fuels, where units cannot be instantly switched on or off due to factors on thermal stress [39, 45]. The switching and up/down time constraints involve discrete variables and this translates the setting into a mixed binary optimization problem in large dimensions [3, 42]. For incorporating transmission constraints, both DC (Direct Current) type approximations and AC (Alternating Current) type formulations have been discussed in literature [38, 40, 41].

The last two decades have seen some focus on increasing the mix of renewable energy into these markets. Renewable energy, though environment friendly comes at an additional cost of uncertainty. Besides generation costs, the other important metrics that have been considered so far in literature are carbon emission levels and penetration levels of renewable energy [51, 52]. These lead to multiobjective versions of the unit commitment problem. For instance [52] and [51] respectively focus on biobjective and triobjective problems with objectives like production costs, maintenance costs, CO₂ emissions, and sulphur emissions. These optimization problems do not generally have a single solution, but a family of solutions, usually denoted by a Pareto-frontier. These solutions represent trade-offs between the multiple objectives of interest. Let $x \in \mathbb{R}^n$ refer to the space of input variables and $f_j : \mathbb{R}^n \rightarrow \mathbb{R}$ represent objective functions for $j = 1, \dots, m$. Then, for any two such Pareto optimal solutions x_1^* and x_2^* (also called non-dominated points), there exist $i, j \in [m] = \{1, \dots, m\}$ such that $f_i(x_1^*) < f_i(x_2^*)$ and $f_j(x_1^*) > f_j(x_2^*)$. The quality of Pareto fronts are usually determined by using the hypervolume metric [2, 50]. More details are listed in the subsequent sections of this work.

*The first author is with Nebenan.de and is reachable at ecetevruez@gmail.com. The second author is the corresponding author and is reachable at both aswin.kannan@hu-berlin.de and aswin.kannan@iiitb.ac.in. This work was done when the first author was pursuing her Masters at Humboldt Universitaet zu Berlin, Germany under the guidance of the second author. The second author was a faculty member and Junior Research Group Leader at Humboldt Universitaet zu Berlin till December 2024. He is currently a faculty member at the International Institute of Information Technology, Bangalore, India (from January 2025). He still retains an affiliation to his Junior Group in Berlin.

In the context of SOUC (Single Objective Unit Commitment), the standard has been to use branch and bound schemes [32,33]. Solvers like `cplex` and `gurobi` use a host of cutting plane type methods [6,13,25,37] and other practical enhancements (includes heuristics) on top of traditional BnB and several other practical enhancements. Other techniques of interest have been genetic algorithms and heuristics that possibly get good lower bounds on the problem [28]. Some approaches consider Lagrangian based schemes, where the coupling constraints are relaxed [3,42]. A detailed test case study of a few heuristics and relaxation based decomposition based for SOUC problems is presented in [23]. Algorithms in the context of MOUC (multiobjective unit commitment) have focused on heuristics and genetic algorithms [21,22,34,46,48,52]. There has been some effort from the standpoint of mathematical programming based approaches [51] for biobjective problems. However, this is a stylized case and centers on a very low dimensional example.

Pareto based avenues to solve multiobjective optimization problems either rely on weights [31] or epsilon constraints [35]. We also specifically note that it has been well accepted in literature that the use of adaptive weights for scalarization [31] is computationally superior in comparison to uniform weights. When the objective functions are nonlinear, using either adaptive weights or epsilon constraints lead to solving mixed-integer optimization problems with nonlinear constraints. Our work proposes the use of McCormick type relaxations to alleviate the difficulty in handling the nonlinear constraints. Our contributions are two fold and are stated as follows.

- **McCormick relaxations:** Along the lines of [1], we consider bi-objective problems (with quadratic objectives) aiming to minimize production costs and carbon emissions. We further note that [1] considers a single objective version of the problem with “unit weights”, while we attempt to compute the Pareto frontier. With the introduction of adaptive weights or epsilon constraints, the resulting sequence of problems present quadratic objectives and quadratic constraints in addition to binary variables and standard linear constraints on startup, capacity, and running conditions. While solvers like `gurobi` handle quadratic constraints, they come at a cost of a huge computational overhead. As the major contribution of this work, we relax such quadratic constraints by means of McCormick relaxations [9,44]. Noting that McCormick relaxations also introduce additional binary variables, we analyze and compare the tradeoffs with solving the quadratically constrained problem. Additionally, it can be observed that the accuracy of our approach depends on the coarseness of McCormick relaxations. We compare solutions and computational overhead across different levels of fineness of McCormick relaxations, with the primitive approach having quadratic constraints. We observe that coarser McCormick relaxations lead to good quality Pareto frontiers for comparatively lower computational budget levels.
- **Practical use case:** We use the practical datasets from [1,51]. This consists of both thermal and hydro generators. We choose a case with 20 thermal and 10 hydro generators. While we consider only two objectives for this work, we note that the framework extends without loss of generality to larger dimensions (in the space of objectives). We plan to investigate along these lines as part of future research.

The rest of the paper is organized into four sections. Section 2 discusses about the basics of multiobjective optimization (MOO) and the formulation specifics related to MOUC. Section 3 proposes the algorithmic framework and the related McCormick relaxations. Section 4 presents numerical results and comparisons on practical test cases from [53]. We conclude in section 5.

2 Basics and Formulation

In this section, we introduce the basics on multiobjective optimization (MOO) and present its mathematical formulation. This is ordered into three subsections, where the first two expand on Pareto solutions and MOO algorithms respectively, while the third portion deals with details of the problem formulation.

2.1 Pareto Optimality

MOO deals with several conflicting objectives simultaneously, leading to a set of solutions with different trade-offs, known as Pareto optimal solutions or non-dominated solutions. In MOO, the goal is to find a balance between conflicting objectives rather than a single optimal solution. This involves two tasks. The former refers to finding Pareto optimal solutions through an optimization process, while the latter points to selecting the most preferred solution based on preferences of the decision-maker (DM). A DM can express preference information, assuming that less is preferred to more for each objective [36]. MOO problems can be mathematically represented as follows [7,31,43].

$$\begin{aligned} & \text{minimize} && F(x) = [f_1(x), f_2(x), \dots, f_k(x)] \\ & \text{subject to} && x \in S, \end{aligned}$$

where $k \geq 2$ and objective functions $f_i : \mathbb{R}^n \rightarrow \mathbb{R}$ are to be minimized simultaneously. The decision variables are denoted by $x \in S \subseteq \mathbb{R}^n$, where S refers to the set of constraints (assumed to be closed and convex throughout the discussion). In MOO, a solution is considered optimal if no component of the objective vector can be improved without worsening at least one other components. A decision vector $x^* \in S$ is **Pareto optimal** if there is no other x in the feasible region such that $f_i(x) \leq f_i(x^*)$ for all $i = 1, \dots, k$ and $f_j(x) < f_j(x^*)$ for at least one index j . We denote the set of Pareto optimal decision vectors by $P(S)$, and the corresponding set of Pareto optimal objective vectors is $P(F)$. We formally define the concept of dominated points and non-dominated solutions as follows.

Definition 1. A point x^a is said to dominate point x^b iff $f_j(x^a) < f_j(x^b)$ for at least one index j and $f_i(x^a) \leq f_i(x^b), \forall i \neq j$. That is,

$$x^a \succ x^b \text{ iff } f_j(x^a) < f_j(x^b) \quad \text{and} \quad f_i(x^a) \leq f_i(x^b).$$

A point x^c is non-dominated iff there exists $j \in \{1, \dots, k\}$ such that $f_j(x^c) < f_j(x)$ for at least one index j and $\forall x \in S$.

The non-dominated set of points constitute the Pareto frontier. To estimate the quality of Pareto frontiers, besides indicators deployed by literature (covered later), the **utopia** and **nadir** points are particularly useful. The **ideal objective vector** $F_{\text{utopia}} \in \mathbb{R}^k$ represents the lower bounds, obtained by minimizing each objective function individually. That is, $F_{\text{utopia}} = [f_1(x^{1,*}), \dots, f_k(x^{k,*})]$, where $x^{i,*} = \operatorname{argmin}_{x \in S} f_i(x)$. Similarly, the **nadir** point refers to the worst case of all the objectives. That is, $F_{\text{nadir}} = [f_1(\hat{x}^1), \dots, f_k(\hat{x}^k)]$, where $\hat{x}^i = \operatorname{argmax}_{x \in S} f_i(x)$.

Hypervolume Indicator: The hypervolume indicator is a widely-used performance metric in multiobjective optimization. This metric measures the volume of the objective space dominated by a set of solutions relative to a reference point [2, 4, 50]. The hypervolume metric provides a single scalar value that reflects both how close the solutions are to the optimal set and how well they are spread out across the objective space simultaneously. Mathematically, given a set of non-dominated solutions S and a reference point r , the hypervolume HV is defined as

$$HV(S, r) = \lambda_n \left(\bigcup_{s \in S} [s; r] \right)$$

where λ_n denotes the n -dimensional Lebesgue measure. The reference point is usually chosen to be dominated by all solutions in the Pareto front. A common practice is to set the reference point slightly worse than the worst value observed in the objective functions across all solutions. While there are other metrics that have been used in literature for quantifying the quality of Pareto solutions, we note that this is beyond the scope of our work. The reader is asked to refer to [2] for more details.

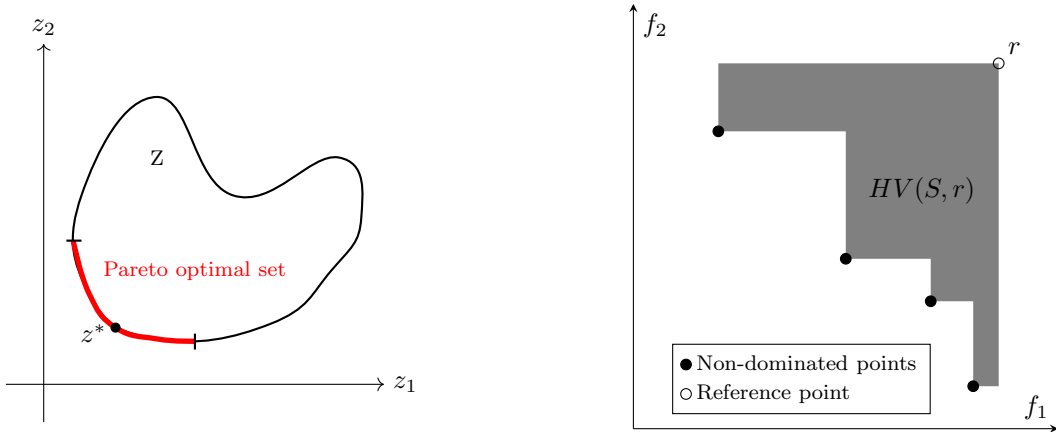


Figure 1: Feasible objective region and Pareto optimal set (Left) and the hypervolume indicator for a bi-objective problem. Plots are self generated.

2.2 MOO Algorithms

In this sub-section, we will discuss about two classic Pareto based methods to solve multiobjective optimization problems. We note that there exist other non-Pareto type methods for MOO like lexicographic techniques. The focus of this paper is however restricted to only Pareto methods.

2.2.1 Weighted Sum Method

This technique focuses on scalarizing the set of objectives into one objective [7, 11, 29]. The process is repeated for multiple choices of such “weights”, which further results in solving a sequence/series of single objective optimization problems.

$$\begin{aligned} \min_x \quad & \sum_{i=1}^k w_i f_i(x) \\ \text{subject to} \quad & x \in S, \end{aligned} \tag{1}$$

where $w_i \geq 0$ for all $i \in \{1, \dots, k\}$ denotes the set of weights and $\sum_{i=1}^k w_i = 1$. Weights can be chosen both in uniform and adaptive ways. Say, as an example for the biobjective case, $w_1 = j/10$ and $w_2 = 1 - w_1$ for $j = \{0, 1, \dots, 10\}$ represents a case with eleven sets of uniform weights. A major disadvantage with uniform weights is that the Pareto frontier may not be uniformly spaced in terms of function values. Recovery of a good Pareto frontier can require many sets of weights and hence can turn out to be computationally expensive. Alternative approaches deploy the concept of adaptive weights [29,31], where weights are sequentially refined based on evaluated objective values. Our framework will focus on adaptive weights and we will discuss more details in the subsequent sections. Pareto frontiers corresponding to MOO problems can be both convex or nonconvex, irrespective of the convexity properties of the objective functions. In nonconvex settings, weighted schemes are not necessarily guaranteed to obtain all points on the Pareto frontier [10]. In these problem instances, the method with epsilon-constraints has proven to be better (to be discussed next).

2.2.2 Epsilon Constraints Method

In this scheme, a sequence of similar single objective optimization problems are solved. However, the objectives are not scalarized using weights. Instead, one objective function is chosen for optimization, while constraints are imposed on the other objectives. This formulation was first presented in [26] and can be stated as follows.

$$\begin{aligned} \text{minimize} \quad & f_i(x) \\ \text{subject to} \quad & f_j(x) \leq \varepsilon_j \quad \text{for all } j = 1, \dots, k, \quad j \neq i, \\ & x \in S. \end{aligned}$$

Note that $i \in \{1, \dots, k\}$ and ε_j are upper bounds for the objectives (with $j \neq i$). A solution $x^* \in S$ is Pareto optimal if and only if it solves the ε -constraint problem for every $l = 1, \dots, k$, where $\varepsilon_j = f_j(x^*)$ for $j = 1, \dots, k$ and $j \neq i$. A unique solution of the ε -constraint problem is Pareto optimal for any upper bounds, which is proven in [36]. Therefore, Pareto optimality either involves solving k different problems (which increases computational cost) or obtaining a unique solution (which can be difficult to verify). A significant advantage of the ε -constraint method is that it does not require the problem to be convex, unlike the weighted sum method. Therefore, it can be used for both convex and non-convex Pareto frontiers [11]. However, choosing the appropriate upper bounds ε_j can be complicated, especially as the number of objective functions increases. If the bounds are not chosen within the minimum and maximum values of each objective function, the feasible region would become empty, and no solution would be found.

2.3 Problem Formulation

We formally describe the problem of interest in this subsection with all the necessary mathematical details. At a very high level, the unit commitment problem is an optimization task in power system operations, where the goal is to determine the optimal schedule for turning power generation units on and off while meeting electricity demand and adhering to various operational constraints [8, 15, 45]. Our focus is on a single firm scenario with a mix of both renewable and non-renewable energy sources. These generators operate over various time intervals, reflecting the need for flexibility and precision in power system operations. Non-renewable units like thermal generators are typically more expensive to operate and emit higher levels of pollutants, but they offer stable and controllable power output. On the other hand, hydro and renewable units, while generally more environment friendly and cost-effective, are subject to variability due to water availability and environmental regulations [27]. We focus on three primary objectives: minimizing operational costs, reducing emissions, and maximizing renewable energy penetration. Each of these objectives is modeled with specific cost functions and constraints, reflecting the economic, environmental, and sustainability goals of the power system. The operational costs include

startup costs, running costs, and generation costs, each modeled to capture the different aspects of power generation economics. Emissions reduction is modeled through quadratic functions of power generation, representing the nonlinear relationship between power output and emissions [52].

Setup and Notation: Let the planning horizon (days or weeks) be denoted by T . Production decisions are determined for discrete time periods t within $\mathcal{T} = \{1, \dots, T\}$, where these intervals can span minutes, hours, or days depending on operational needs and grid demands. The firm operates multiple generators, indexed by $\mathcal{I} = \{1, \dots, I\}$, where each generator can be in an operational state of either being on or off. Once the decision to activate or deactivate a generator is made, these are constrained by minimum up time and down time due to factors like thermal stresses and the need for equipment to cool down or warm up [39, 45]. The decision variables determine the operational status of each unit within the system, the amount of power generated, and the startup and shutdown activities over the planning horizon. Specifically, for each generator i and time t , we define:

- y_{it} - a binary variable representing whether unit i is started ($y_{it} = 1$) or not ($y_{it} = 0$) at time t .
- z_{it} - a binary variable representing whether unit i is on ($z_{it} = 1$) or off ($z_{it} = 0$) at time t .
- g_{it} - a continuous variable representing the amount of power generated by unit i at time t .

2.3.1 Objective Functions

We consider objectives that reflect broader goals of economic efficiency and environmental sustainability. These can be broadly classified as follows.

Generation Costs: The operational costs for power generation are multifaceted and can be categorized into three primary types [18, 23, 24, 52]:

- **Startup Costs:** These costs are incurred each time a generator is switched from the off mode to on. This transition often requires a significant amount of fuel and power, especially for thermal units. The startup costs are modeled as a linear function of the binary decision variable y_{it} , which indicates whether unit i is started ($y_{it} = 1$) at time t .
- **Running Costs:** These are the costs associated with keeping a generator in an operational state, regardless of the actual power generation. This includes costs for idling, where the generator is on but not necessarily producing power. The running costs are modeled as a linear function tied to the binary variable z_{it} .
- **Generation Costs:** These costs are directly related to the amount of electricity generated by each unit. Specifically, generation costs are modeled as a quadratic function of the power output.

The total generation cost for the utility is the aggregate of all these individual costs across all units and time periods, formulated as:

$$f_c(y, z, g) = \sum_{i \in \mathcal{I}} \sum_{t \in \mathcal{T}} (f_{it}^y(y_{it}) + f_{it}^z(z_{it}) + f_{it}^g(g_{it})), \quad (2)$$

where $f_{it}^y(\cdot)$, $f_{it}^z(\cdot)$, and $f_{it}^g(\cdot)$ represent the cost functions for startup, running, and generation, respectively.

Emissions: Regulatory requirements on environmental aspects require emissions from CO₂ and sulfur to be maintained at lower levels. These emissions are particularly more when generating power from coal and oil based generators. In sync with previous literature, we model the emission levels (Tons/Kgs of CO₂) by means of quadratic functions. These costs are encapsulated using coefficients $\alpha > 0$ and $\beta > 0$, which vary based on the fuel type and technology of the generator. The mathematical representation of the emissions objective is:

$$f_e = \sum_{i \in \mathcal{I}} \sum_{t \in \mathcal{T}} (\beta_{it} g_{it} + \gamma_{it} g_{it}^2). \quad (3)$$

Renewable Energy Penetration: This objective aims to maximize the contribution of renewable sources like wind and solar relative to conventional fossil-fuel-based generation. This is critical for transitioning towards a more sustainable and less carbon-intensive power grid. The goal can be expressed either as a direct maximization of renewable output or as an optimization of the ratio of renewable to non-renewable generation. The formulations for these objectives are as follows.

$$f_r = - \sum_{t \in \mathcal{T}} \left(\sum_{i \in \mathcal{I}_c} g_{it} - \sum_{i \in \mathcal{I}_r} g_{it} \right) \quad \text{or alternatively,} \quad f_r = \frac{\sum_{t \in \mathcal{T}} \sum_{i \in \mathcal{I}_r} g_{it}}{\sum_{t \in \mathcal{T}} \sum_{i \in \mathcal{I}_c} g_{it}}. \quad (4)$$

Note that \mathcal{I}_r and \mathcal{I}_c denote the sets of renewable and conventional generators, respectively.

2.3.2 Constraints

The unit commitment problem involves a variety of constraints that ensure the feasibility and reliability of power generation schedules. These constraints cover aspects such as startup and shutdown protocols, generation limits, and the need to meet electricity demand at all times. Below, we detail the key constraints incorporated into our model. As a simple example, let's take the case of coal generators. Once these coal units are switched on, they need to be running for a certain amount of time before being turned off. On a similar note, units cannot be turned on immediately after they are turned off. These are collectively modeled by means of startup and running variables.

Startup and Shutdown Constraints: The relationship between startup variables y and running variables z is crucial for accurately modeling the operational dynamics of power units [17, 23]. If a unit is off at time t (i.e. $z_{it} = 0$) and switched on at time $t + 1$ (i.e. $z_{it} = 1$), then $y_{i,t+1}$ is 1. In all other scenarios, $y_{i,t+1}$ is 0. The relationship between startup and running states can be expressed as:

$$y_{it} = \max(z_{it} - z_{i,t-1}, 0). \quad (5)$$

Given our assumptions on $f^y(\cdot)$ being convex, increasing, and positive, (5) can be formulated as follows.

$$y_{it} \geq z_{it} - z_{i,t-1}, \quad y_{it} \geq 0. \quad (6)$$

Up and Down Time Constraints: As mentioned earlier, once a unit is turned on, it must remain on for a few time periods (up-time), and similarly, once turned off, it must remain off for some time (down-time). Let the respective "minimum" up and down times be denoted by L_i and l_i . The related constraints can be modeled as follows. For more details on such models, the reader is asked to refer to [12, 24].

$$z_{it} - z_{i,t-1} \leq z_{i,\tau}, \quad \forall t \in \mathcal{T}, \forall \tau \in \{t + 1, \dots, \min(t + L_i - 1, T)\}, \quad (7)$$

$$z_{i,t-1} - z_{it} \leq 1 - z_{i,\tau}, \quad \forall t \in \mathcal{T}, \forall \tau \in \{t + 1, \dots, \min(t + l_i - 1, T)\}. \quad (8)$$

Generation Constraints: Each generator has specific operational limits defined by its minimum and maximum generation levels, denoted by q_i and Q_i , respectively. A unit can only produce power when it is on, thus the generation levels must be bounded by these limits and can be expressed as follows.

$$q_i z_{it} \leq g_{it} \leq Q_i z_{it}, \quad \forall i \in \mathcal{I}, \forall t \in \mathcal{T}. \quad (9)$$

In this work, we do not consider ramp constraints. Note that these constraints can be easily embedded into our model without loss of generality.

Demand Constraints: In addition to individual generator limits, the total power generated at each time step must meet or exceed the electricity demand. This requirement is crucial for maintaining grid stability and is represented by the following constraint.

$$\sum_{i=1}^I g_{it} \geq d_t, \quad \forall t \in \mathcal{T}. \quad (10)$$

2.3.3 Mathematical representation in matrix form

For the ease of parsing, we transform our formulation into a matrix notation. The MOUC hence can be put forth as follows.

$$\begin{aligned} \min_{y,z,g} \quad & F(y, z, g) = [f_c(y, z, g), f_e(g), f_r(g)] \\ \text{subject to} \quad & \{y, z, g\} \in \mathcal{X}, \end{aligned} \quad (11)$$

where $F(y, z, g)$ encompasses the cost, emission, and renewable energy penetration objectives. The feasible region \mathcal{X} is defined by the intersection of the startup, shutdown, up and down time constraints, generation capacities, and demand constraints.

$$\mathcal{X} = \{x_b, g \mid A_b x_b + Bg \leq u, Dg \leq v, Ex_b \leq v, x_b \in \{0, 1\}\}, \quad (12)$$

where the matrices A_b , B , D , and E encode the relationships and bounds of the variables. The specific elements of these matrices are defined as follows:

$$x_b = \begin{pmatrix} y \\ z \end{pmatrix}, g = \begin{pmatrix} g_1 \\ \vdots \\ g_T \end{pmatrix}, z = \begin{pmatrix} z_{11} \\ \vdots \\ z_{1T} \\ \vdots \\ z_{IT} \end{pmatrix}, A_b = \begin{pmatrix} 0 & q_1 I \\ \vdots & \vdots \\ 0 & q_T I \\ 0 & -Q_1 I \\ \vdots & \vdots \\ 0 & -Q_I I \end{pmatrix}, B = \begin{pmatrix} -I & \cdots & 0 \\ \vdots & \ddots & \vdots \\ 0 & \cdots & -I \\ I & \cdots & 0 \\ \vdots & \ddots & \vdots \\ 0 & \cdots & I \end{pmatrix},$$

$$D = (I \quad \cdots \quad I), u = \begin{pmatrix} d_1 \\ \vdots \\ d_T \end{pmatrix}, E = \begin{pmatrix} E_1 \\ E_2 \\ -E_2 \end{pmatrix}, E_1 = \begin{pmatrix} -1 & 1 & \cdots & 0 & 0 & -1 & \cdots & 0 \\ \vdots & \vdots & \ddots & \vdots & \vdots & \vdots & \ddots & \vdots \\ 0 & \cdots & -1 & 1 & 0 & 0 & \cdots & -1 \end{pmatrix}.$$

For the sake of simplicity, the set \mathcal{X} can be further denoted as follows. Note that we use the following notation for the rest of our paper.

$$\mathcal{X} = \{x | Ax \leq b, x_b \in \{0, 1\}\}, x = \begin{pmatrix} g \\ x_b \end{pmatrix}. \quad (13)$$

3 Algorithms

As stated earlier in section 1, the MOUC has received less interest from the standpoint of Mathematical programming based approaches. One of the key reasons for the same is that the computational complexity of these schemes increases significantly as the problem dimension grows, especially when dealing with both continuous and integer variables. One major challenge is that using uniform weights to generate a reasonable Pareto frontier requires evaluating an enormous number of weight combinations. For a detailed discussion of this complexity, the reader is referred to previous works [29–31]. The use of adaptive weights [30] on the other hand requires lesser number of weight combinations. However, using adaptive weights leads to some complexity due to the introduction of nonlinear constraints into the problem. To alleviate the issue of nonlinear constraints, we propose using McCormick-type relaxations, which approximate the feasible space by applying linear envelopes. This approach is discussed in more detail in the following subsections.

3.1 Adaptive Weighted Sum (AWS) Method

In this work, we focus only on bi-objective problems. The AWS method begins with an initial step similar to the traditional weighted-sum approach but with a large step size for the weighting factor, λ . This initial step generates a coarse representation of the Pareto front. The method then identifies regions that need further refinement by calculating distances between neighboring solutions. These identified regions are targeted for sub-optimization with additional inequality constraints. The process is repeated iteratively, refining the Pareto front until a pre-specified resolution is achieved. We summarize the method of adaptive weights from [30] for the case of two objectives in figure 2. This is subsequently explained stepwise in algorithm .1.

Stepwise description of the algorithm: Algorithm .1 can be further elaborated as follows.

- **Initial Weighted-Sum Optimization:** This starts with a traditional weighted-sum approach to multiobjective optimization, using a small number of weight combinations n_{initial} and a large step size ($\Delta\lambda$),

$$\Delta\lambda = \frac{1}{n_{\text{initial}}}.$$

- **Segment Length Calculation:** This step calculates the Euclidean distances between neighboring solutions to identify segments needing refinement. In process, nearly overlapping solutions, where inter-segment lengths less than a prescribed threshold ϵ , are removed.
- **Determination of Further Refinements:** The number of further refinements (n_i) is determined for each segment based on its length relative to the average length of the segment as follows.

$$n_i = \text{round} \left(C \frac{l_i}{l_{\text{avg}}} \right),$$

Note that l_i is the length of the i -th segment, l_{avg} is the average segment length, and C is a constant. If $n_i \leq 1$, there is no further refinement needed for the i -th segment. Else, the algorithm proceeds with the following step.

Algorithm .1 Adaptive Weighted-Sum Method (AWS)

- 1: **Input:** Objective functions f_i , initial parameters δ_J (distance threshold), ε (tolerance), C (scaling factor), n_{initial} (initial number of solutions)
 - 2: **Output:** Refined Pareto front
 - 3: **Normalize Objective Functions:**
 - 4: **for** each objective function f_i **do**
 - 5: Compute $f_i^* = \frac{f_i - f_i^U}{f_i^N - f_i^U}$ ▷ Normalize objective functions
 - 6: **end for**
 - 7: **Initial Weighted-Sum Optimization:**
 - 8: Perform weighted-sum optimization with step size $\Delta\lambda = \frac{1}{n_{\text{initial}}}$.
 - 9: **repeat**
 - 10: **Segment Length Calculation:**
 - 11: **for** each neighboring solution pair **do**
 - 12: Calculate Euclidean distance l_i between the two solutions
 - 13: **if** $l_i < \varepsilon$ **then**
 - 14: Remove overlapping solution ▷ Remove solutions that are too close (overlap)
 - 15: **end if**
 - 16: **end for**
 - 17: **Determination of Further Refinements:**
 - 18: **for** each segment i **do**
 - 19: Compute $n_i = \text{round} \left(C \frac{l_i}{\text{avg}} \right)$
 - 20: **if** $n_i > 1$ **then**
 - 21: **Calculation of the Offset Distances:**
 - 22: Compute $\theta = \tan^{-1} \left(-\frac{P_1^y - P_2^y}{P_1^x - P_2^x} \right)$
 - 23: Compute $\delta_1 = \delta_J \cos \theta$, $\delta_2 = \delta_J \sin \theta$
 - 24: **Sub-Optimization with Additional Constraints:**
 - 25: Perform optimization with additional constraints and n_i weighted pairs:
$$\begin{aligned} & \min_x \lambda f_1(x) + (1 - \lambda) f_2(x) \\ & \text{s.t.} \\ & f_1(x) \leq P_1^x - \delta_1 \\ & f_2(x) \leq P_2^y - \delta_2 \\ & \lambda \in [0, 1] \end{aligned}$$
 - 26: **end if**
 - 27: **end for**
 - 28: **Iteration and Termination:**
 - 29: Compute lengths of new segments and remove overlapping solutions
 - 30: **until** all segment lengths are below δ_J
-

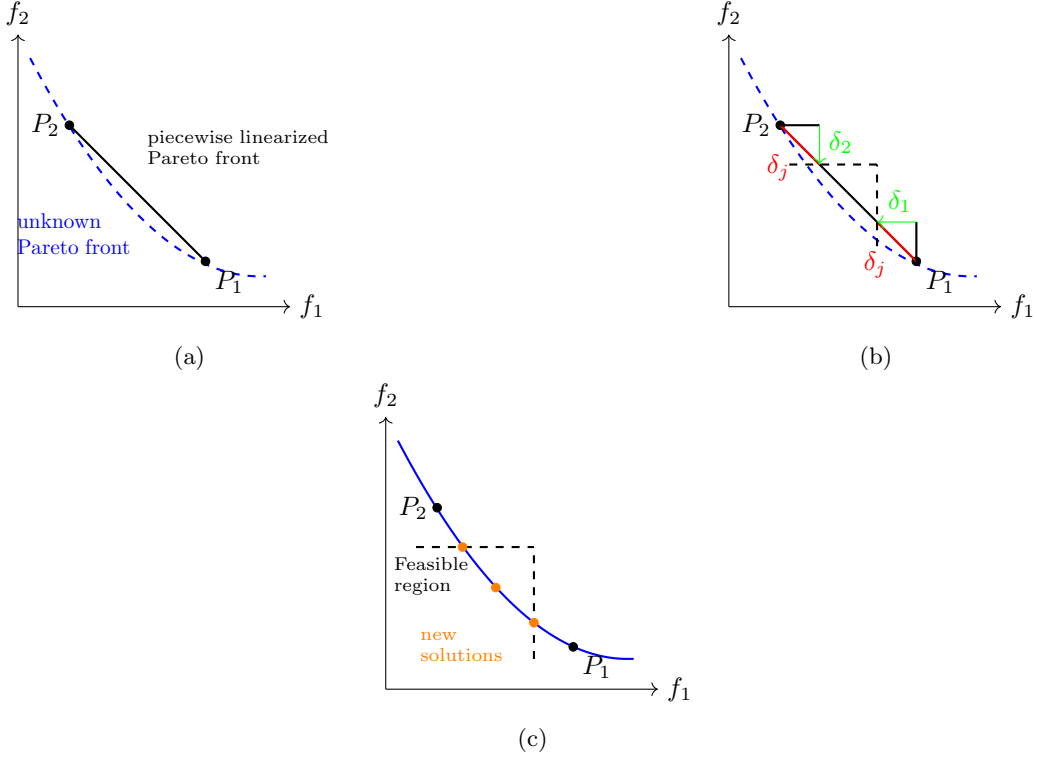


Figure 2: The offset distances, δ_1 and δ_2

- Calculation of the Offset Distances: For segments needing further refinement, the offset distances (δ_1 and δ_2) are calculated from the segment endpoints in the direction of the objective functions. Here, δ_J is the prescribed maximum length for segment refinement, and P_1^x, P_2^x, P_1^y , and P_2^y are the coordinates of the endpoints of the segment in the objective space. The offset distances are calculated using the angle θ between the segment and the objective axes as follows.

$$\theta = \tan^{-1} \left(-\frac{P_1^y - P_2^y}{P_1^x - P_2^x} \right)$$

$$\delta_1 = \delta_J \cos \theta, \quad \delta_2 = \delta_J \sin \theta$$

- Sub-Optimization with Additional Constraints: Based on the calculated offset distances, additional inequality constraints are imposed and the following optimization subproblem is solved. Note that $\lambda \in [0, 1]$.

$$\begin{aligned} \min_x \quad & \lambda f_1(x) + (1 - \lambda) f_2(x) \\ \text{s.t.} \quad & f_1(x) \leq P_1^x - \delta_1 \\ & f_2(x) \leq P_2^y - \delta_2. \end{aligned}$$

Segments that do not converge to optimal solutions are excluded from further refinement, as they correspond to non-convex regions that do not contain Pareto optimal solutions.

- Iteration and Termination: Calculate the lengths of the new segments and eliminate nearly overlapping solutions. Continue the refinement process until all segment lengths are reduced to below the specified maximum threshold δ_J .

Without loss of generality, this can be extended to more objectives by fixing the weights of all but two objectives. One such generalization is presented in [31].

Parameter Selection: The Adaptive Weighted-Sum (AWS) method involves several key parameters that must be carefully set to ensure effective optimization. These parameters are the offset distance, the Euclidean distance for determining overlapping solutions, the constant for further refinement (C), and the number of Pareto front segments in the initial iteration (n_{initial}). These parameters influence the refinement process and the distribution of solutions along the Pareto front. The Adaptive Weighted-Sum (AWS) method involves several key parameters that significantly impact optimization performance.

These include the offset distance (δ_J), the Euclidean distance for identifying overlapping solutions (ϵ), the refinement constant (C), and the number of initial Pareto front segments n_{initial} . Each of these parameters governs the refinement process and the distribution of solutions along the Pareto front. Succinctly, this can be put forth as follows.

- δ_J must be small to produce denser solutions. It is typically set between 0.05 and 0.2 in the space of normalized objectives.
- ϵ must be smaller than δ_J to ensure accurate segmentation.
- C being too small prevents further refinement. Large values of C result in excessive overlapping solutions, further increasing the computational cost.
- n_{initial} : Here, a balance is needed. Too few divisions may hinder refinement in later stages, while too many can increase computational burden. A typical range of 3 to 10 divisions is recommended.

3.2 McCormick Relaxation

McCormick envelopes facilitate the computation of solutions to complex optimization problems with bilinear structure by approximating them with linear constraints [9, 47]. The use of such relaxations have been common from the standpoint of continuous optimization problems. Moreover, theoretically it has been established in [5, 47] that McCormick relaxation of the product of two functions can achieve quadratic convergence under certain conditions. For our problem of interest, we present McCormick relaxations in two levels of granularity.

3.2.1 Single-Layer McCormick Relaxation

These form the foundation of the relaxations and these are the weakest version of the approximations. Consider a bilinear term $w = xy$, where x and y are bounded by $x \in [x_L, x_U]$ and $y \in [y_L, y_U]$. Along the lines of [14], the relaxation can be constructed using the following linear inequalities.

1. Consider $a = (x - x^L)$ and $b = (y - y^L)$. Since both a and b are non-negative:

$$a \cdot b \geq 0 \implies (x - x^L)(y - y^L) = xy - x^L y - xy^L + x^L y^L \geq 0$$

Rearranging, we obtain:

$$w \geq x^L y + xy^L - x^L y^L$$

2. Consider $a = (x^U - x)$ and $b = (y^U - y)$. Again, since a and b are non-negative:

$$a \cdot b \geq 0 \implies (x^U - x)(y^U - y) = x^U y^U - x^U y - xy^U + xy \geq 0$$

Rearranging, we obtain:

$$w \leq x^U y + xy^U - x^U y^U$$

3. Considering $a = (x^U - x)$ and $b = (y - y^L)$, we obtain analogously:

$$w \leq x^U y + xy^L - x^U y^L$$

4. Lastly, considering $a = (x - x^L)$ and $b = (y^U - y)$ we obtain:

$$w \leq xy^U + x^L y - x^L y^U$$

More concisely, $w = xy$ can further be represented by the **underestimators**:

$$\begin{aligned} w &\geq x^L y + xy^L - x^L y^L, \\ w &\geq x^U y + xy^U - x^U y^U \end{aligned}$$

and the **overestimators**:

$$\begin{aligned} w &\leq x^U y + xy^L - x^U y^L, \\ w &\leq xy^U + x^L y - x^L y^U. \end{aligned}$$

The primary advantage as it can be easily noticed is that the original nonconvex constraints are relaxed by means of convex and linear inequalities. This helps significantly with computational tractability of the problem. The accuracy and tightness of this relaxation remains a question. The next subsection discusses on a more close examination of the same. Our empirical results (discussed later) will cover this in detail.

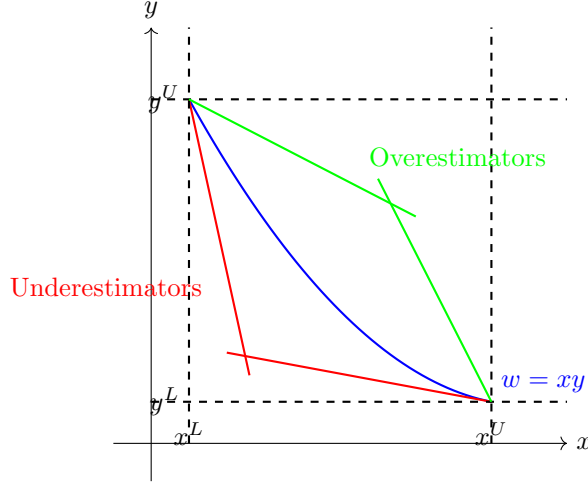


Figure 3: McCormick Envelopes with Underestimators and Overestimators

3.2.2 Multi-Layer McCormick Relaxation

These are higher order generalizations, where the domain of the variables is partitioned into multiple segments [9]. This yields tighter envelopes. However, such a partitioning also has a disadvantage in that these envelopes are piecewise linear and therefore involve additional binary variables to be introduced into the formulation.

Consider the bilinear term $w = xy$ with x and y bounded by $x \in [x^L, x^U]$ and $y \in [y^L, y^U]$ as earlier. To apply a multi-layer McCormick relaxation, the domain of x is partitioned into N intervals $[x_n^L, x_n^U]$ and the bounds for $[y_n^L, y_n^U]$ are adjusted accordingly. Additionally, binary variables q_n and a large constant M are introduced into the formulation to accommodate for multiple such piecewise envelopes. Here, the variable q_n corresponding to the n th piece takes the value of “1” if the variable “ w ” is in piece (partition) “ n ” and 0 otherwise. The envelopes for partition n are hence constructed as follows.

$$\begin{aligned}
 w &\geq x_n^L y + x y_n^L - x_n^L y_n^L - (1 - q_n)M, & \text{Underestimator 1} \\
 w &\geq x_n^U y + x y_n^U - x_n^U y_n^U - (1 - q_n)M, & \text{Underestimator 2} \\
 w &\leq x_n^U y + x y_n^L - x_n^U y_n^L + (1 - q_n)M, & \text{Overestimator 1} \\
 w &\leq x_n^L y + x y_n^U - x_n^L y_n^U + (1 - q_n)M, & \text{Overestimator 2} \\
 q_n &\in \{0, 1\}, \quad \sum_n^N q_n = 1.
 \end{aligned}$$

The partitions in the multi-layer McCormick relaxation can be uniform or non-uniform. In the case of uniform partitions, the bounds for x in each partition n can be defined as follows:

$$\begin{aligned}
 x_1^L &= x^L, \quad x_N^U = x^U \\
 x_n^L &= x_{n-1}^U, \quad \text{for } n = 2, 3, \dots, N, \\
 x_n^U &= x^L + n \frac{x^U - x^L}{N}, \quad \text{for } n = 1, 2, \dots, N - 1.
 \end{aligned}$$

The bounds for $[y_n^L, y_n^U]$ are adjusted accordingly. According to [9], multi-layer McCormick relaxation significantly improves the quality of the relaxation and reduces the optimality gap in large-scale optimization problems. This iterative approach allows for better handling of complex constraints and objectives, making it a valuable tool in the context of unit commitment.

3.3 Adaptation of McCormick Relaxations to MOUC

For completeness, in this section, we expand on the details of the formulation of the McCormick relaxations, when specifically applied to our algorithm with AWS and epsilon constraints.

3.3.1 Adaptive Weights (AWS)

We begin with AWS and present the formulation with McCormick relaxations for two levels of granularity.

Single Layer McCormick: Consider the matrices Q_1 and Q_2 stated earlier. For the ease of computation, we marginally regularize the matrices by adding a term ϵI to both matrices. Note that I refers to an identity matrix and ϵ was set to be 0.01 times the average value of the elements in $|Q_1|$ and $|Q_2|$. Note that $|\cdot|$ denotes the absolute value function. The formulation further involves the following steps.

- **Cholesky decomposition:** The regularized matrices Q_1 and Q_2 are factorized using Cholesky decomposition. This results in lower triangular matrices L_1 and L_2 , such that $Q_1 = L_1 * L_1^T$, $Q_2 = L_2 * L_2^T$.
- **Setting variable bounds:** The upper bounds x_U on the decision variables are determined based on the maximum power for continuous variables and are set to ones for binary variables. The lower bounds x_L are set to zero. For completeness, $x^L \leq x \leq x^U$.
- **Auxiliary Variables:** Auxiliary variables y_1 , y_2 , w_1 , and w_2 are introduced such that

$$e^T w_1 = y_1^T y_1 = \sum_{i=1}^n (y_{1,i})^2, w_{1,i} = y_{1,i}^2, \forall i = 1 \dots n, \quad (14)$$

$$e^T w_2 = y_2^T y_2 = \sum_{i=1}^n (y_{2,i})^2, w_{2,i} = y_{2,i}^2, \forall i = 1 \dots n. \quad (15)$$

The variables y_1, y_2 and the bounds on the same are given as follows.

$$y_1 = L_1^T x \quad \text{and} \quad y_2 = L_2^T x.$$

$$y_1^U = L_1^T x^U, y_1^L = L_1^T x^L, y_2^U = L_2^T x^U, \quad \text{and} \quad y_2^L = L_2^T x^L.$$

Therefore, the constraints marking the refinements can be further expressed as follows. Note that e refers to a vector of ones.

$$e^T w_1 + \text{lin}_1^T x \leq P_1^x - \delta_1 \quad \text{and} \quad e^T w_2 + \text{lin}_2^T x \leq P_2^y - \delta_2. \quad (16)$$

By relaxing $w_{1,i} = y_{1,i}^2$ for all $i = 1, \dots, n$ and $w_{2,i} = y_{2,i}^2 \forall i = 1, \dots, n$ using a single-layer McCormick relaxation, we obtain the following optimization problem with linearized constraints. Note that $\lambda \in [0, 1]$ as earlier.

$$\begin{aligned} & \min_x \lambda f_1(x) + (1 - \lambda) f_2(x) \\ & \text{subject to: } Ax \leq b, x_b \in \{0, 1\}^{2IT}, x_L \leq x \leq x_U, && \text{(original constraints)} \\ & e^T w_1 + \text{lin}_1^T x \leq P_1^x - \delta_1, \quad e^T w_2 + \text{lin}_2^T x \leq P_2^y - \delta_2, && \text{(additional constraints)} \\ & w_1 \geq 2y_1 y_1^L - (y_1^L)^2, && \text{(underestimator for } f_1) \\ & w_1 \geq 2y_1 y_1^U - (y_1^U)^2, && \text{(underestimator for } f_1) \\ & w_1 \leq y_1(y_1^L + y_1^U) - y_1^U y_1^L, && \text{(overestimator for } f_1) \\ & w_2 \geq 2y_2 y_2^L - (y_2^L)^2, && \text{(underestimator for } f_2) \\ & w_2 \geq 2y_2 y_2^U - (y_2^U)^2, && \text{(underestimator for } f_2) \\ & w_2 \leq y_2(y_2^L + y_2^U) - y_2^U y_2^L, && \text{(overestimator for } f_2) \\ & y_1 = L_1^T x, \quad y_2 = L_2^T x, && \text{(others)}. \end{aligned}$$

Therefore, the linearized constraints can be incorporated into the optimization model, resulting in a new set of constraints $A_{\text{mck1}} \cdot x \leq b_{\text{mck1}}$, where:

$$A_{\text{mck1}} = \begin{pmatrix} A & \mathbf{0} & \mathbf{0} & \mathbf{0} & \mathbf{0} \\ \text{lin}_1^T & \mathbf{0} & \mathbf{0} & \mathbf{1} & \mathbf{0} \\ \text{lin}_2^T & \mathbf{0} & \mathbf{0} & \mathbf{0} & \mathbf{1} \\ \mathbf{0} & 2 \cdot \text{diag}(y_1^L) & \mathbf{0} & -\mathbf{I} & \mathbf{0} \\ \mathbf{0} & 2 \cdot \text{diag}(y_1^U) & \mathbf{0} & -\mathbf{I} & \mathbf{0} \\ \mathbf{0} & \text{diag}(-(y_1^U + y_1^L)) & \mathbf{0} & \mathbf{I} & \mathbf{0} \\ \mathbf{0} & \mathbf{0} & 2 \cdot \text{diag}(y_2^L) & \mathbf{0} & -\mathbf{I} \\ \mathbf{0} & \mathbf{0} & 2 \cdot \text{diag}(y_2^U) & \mathbf{0} & -\mathbf{I} \\ \mathbf{0} & \mathbf{0} & \text{diag}(-(y_2^U + y_2^L)) & \mathbf{0} & \mathbf{I} \\ L_1^T & -\mathbf{I} & \mathbf{0} & \mathbf{0} & \mathbf{0} \\ L_2^T & \mathbf{0} & -\mathbf{I} & \mathbf{0} & \mathbf{0} \end{pmatrix}, \quad b_{\text{mck1}} = \begin{pmatrix} b \\ P_1^x - \delta_1 \\ P_2^y - \delta_2 \\ y_1^L \cdot y_1^L \\ y_1^U \cdot y_1^U \\ -(y_1^U \cdot y_1^L) \\ y_2^L \cdot y_2^L \\ y_2^U \cdot y_2^U \\ -(y_2^U \cdot y_2^L) \\ \mathbf{0} \\ \mathbf{0} \end{pmatrix}.$$

In this optimization problem with linearized constraints, the number of decision variables increases from n to $5n$ due to the inclusion of auxiliary variables y_1 , y_2 , w_1 , and w_2 alongside the original decision variables x .

Two Layer McCormick: In this case, the bounds for y_1 and y_2 are divided into two pieces as follows.

$$\begin{aligned} y_{1a}^L &= y_1^L, & y_{1a}^U &= \frac{y_1^U + y_1^L}{2}, & y_{1b}^L &= y_{1a}^U, & y_{1b}^U &= y_1^U, \\ y_{2a}^L &= y_2^L, & y_{2a}^U &= \frac{y_2^U + y_2^L}{2}, & y_{2b}^L &= y_{2a}^U, & y_{2b}^U &= y_2^U. \end{aligned}$$

Additionally, we introduce binary variables q_a and q_b , corresponding to the pieces a and b , where $q_a, q_b \in \{0, 1\}$ and $q_a + q_b = 1 \forall i = 1, \dots, n$, indicating that only one of the pieces a or b is active at a time. Therefore, by relaxing $w_{1,i} = y_{1,i}^2 \forall i = 1, \dots, n$ and $w_{2,i} = y_{2,i}^2 \forall i = 1, \dots, n$ using a two-layer McCormick relaxation, we obtain the following optimization problem with linearized constraints.

$$\begin{aligned} \min_x \quad & \lambda f_1(x) + (1 - \lambda) f_2(x) \\ \text{subject to:} \quad & Ax \leq b, \quad x_b \in \{0, 1\}^{2IT}, \quad x_L \leq x \leq x_U, & (\text{original constraints}) \\ & e^T w_1 + \text{lin}_1^T x \leq P_1^x - \delta_1, \quad e^T w_2 + \text{lin}_2^T x \leq P_2^y - \delta_2, \\ & w_1 \geq 2y_1 y_{1a}^L - (y_{1a}^L)^2 - (1 - q_a)M, \\ & w_1 \geq 2y_1 y_{1a}^U - (y_{1a}^U)^2 - (1 - q_a)M, \\ & w_1 \leq y_1(y_{1a}^L + y_{1a}^U) - y_{1a}^U y_{1a}^L + (1 - q_a)M, \\ & w_2 \geq 2y_2 y_{2a}^L - (y_{2a}^L)^2 - (1 - q_a)M, \\ & w_2 \geq 2y_2 y_{2a}^U - (y_{2a}^U)^2 - (1 - q_a)M, \\ & w_2 \leq y_2(y_{2a}^L + y_{2a}^U) - y_{2a}^U y_{2a}^L + (1 - q_a)M, \\ & w_1 \geq 2y_1 y_{1b}^L - (y_{1b}^L)^2 - (1 - q_b)M, \\ & w_1 \geq 2y_1 y_{1b}^U - (y_{1b}^U)^2 - (1 - q_b)M, \\ & w_1 \leq y_1(y_{1b}^L + y_{1b}^U) - y_{1b}^U y_{1b}^L + (1 - q_b)M, \\ & w_2 \geq 2y_2 y_{2b}^L - (y_{2b}^L)^2 - (1 - q_b)M, \\ & w_2 \geq 2y_2 y_{2b}^U - (y_{2b}^U)^2 - (1 - q_b)M, \\ & w_2 \leq y_2(y_{2b}^L + y_{2b}^U) - y_{2b}^U y_{2b}^L + (1 - q_b)M, \\ & q_a \in \{0, 1\}, q_b \in \{0, 1\}, \quad q_a + q_b = 1. \end{aligned}$$

Note that M is a scalar big enough to deactivate a set of constraints when either $q_{a,i} = 0$ or $q_{b,i} = 0$. Therefore, this results in a new set of constraints $A_{\text{mck2}} \cdot x \leq b_{\text{mck2}}$, where:

$$A_{\text{mck2}} = \begin{pmatrix} A & \mathbf{0} & \mathbf{0} & \mathbf{0} & \mathbf{0} & \mathbf{0} & \mathbf{0} \\ \text{lin}_1^T & \mathbf{0} & \mathbf{0} & \mathbf{1} & \mathbf{0} & \mathbf{0} & \mathbf{0} \\ \text{lin}_2^T & \mathbf{0} & \mathbf{0} & \mathbf{0} & \mathbf{1} & \mathbf{0} & \mathbf{0} \\ \mathbf{0} & 2 \cdot \text{diag}(y_{1a}^L) & \mathbf{0} & -\mathbf{I} & \mathbf{0} & M \cdot \mathbf{I} & \mathbf{0} \\ \mathbf{0} & 2 \cdot \text{diag}(y_{1a}^U) & \mathbf{0} & -\mathbf{I} & \mathbf{0} & M \cdot \mathbf{I} & \mathbf{0} \\ \mathbf{0} & \text{diag}(-(y_{1a}^U + y_{1a}^L)) & \mathbf{0} & \mathbf{I} & \mathbf{0} & M \cdot \mathbf{I} & \mathbf{0} \\ \mathbf{0} & \mathbf{0} & 2 \cdot \text{diag}(y_{2a}^L) & \mathbf{0} & -\mathbf{I} & M \cdot \mathbf{I} & \mathbf{0} \\ \mathbf{0} & \mathbf{0} & 2 \cdot \text{diag}(y_{2a}^U) & \mathbf{0} & -\mathbf{I} & M \cdot \mathbf{I} & \mathbf{0} \\ \mathbf{0} & \mathbf{0} & \text{diag}(-(y_{2a}^U + y_{2a}^L)) & \mathbf{0} & \mathbf{I} & M \cdot \mathbf{I} & \mathbf{0} \\ \mathbf{0} & 2 \cdot \text{diag}(y_{1b}^L) & \mathbf{0} & -\mathbf{I} & \mathbf{0} & M \cdot \mathbf{I} & \mathbf{0} \\ \mathbf{0} & 2 \cdot \text{diag}(y_{1b}^U) & \mathbf{0} & -\mathbf{I} & \mathbf{0} & M \cdot \mathbf{I} & \mathbf{0} \\ \mathbf{0} & \text{diag}(-(y_{1b}^U + y_{1b}^L)) & \mathbf{0} & \mathbf{I} & \mathbf{0} & M \cdot \mathbf{I} & \mathbf{0} \\ \mathbf{0} & \mathbf{0} & 2 \cdot \text{diag}(y_{2b}^L) & \mathbf{0} & -\mathbf{I} & M \cdot \mathbf{I} & \mathbf{0} \\ \mathbf{0} & \mathbf{0} & 2 \cdot \text{diag}(y_{2b}^U) & \mathbf{0} & -\mathbf{I} & M \cdot \mathbf{I} & \mathbf{0} \\ \mathbf{0} & \mathbf{0} & \text{diag}(-(y_{2b}^U + y_{2b}^L)) & \mathbf{0} & \mathbf{I} & M \cdot \mathbf{I} & \mathbf{0} \\ L_1^T & -\mathbf{I} & \mathbf{0} & \mathbf{0} & \mathbf{0} & \mathbf{0} & \mathbf{0} \\ L_2^T & \mathbf{0} & -\mathbf{I} & \mathbf{0} & \mathbf{0} & \mathbf{0} & \mathbf{0} \\ \mathbf{0} & \mathbf{0} & \mathbf{0} & \mathbf{0} & \mathbf{0} & \mathbf{I} & \mathbf{I} \end{pmatrix}, \quad b_{\text{mck2}} = \begin{pmatrix} b \\ P_1^x - \delta_1 \\ P_2^y - \delta_2 \\ (y_{1a}^L)^2 + M \cdot \mathbf{1} \\ (y_{1a}^U)^2 + M \cdot \mathbf{1} \\ (y_{1a}^L)^2 + M \cdot \mathbf{1} \\ -(y_{1a}^U \cdot y_{1a}^L) + M \cdot \mathbf{1} \\ (y_{2a}^L)^2 + M \cdot \mathbf{1} \\ (y_{2a}^U)^2 + M \cdot \mathbf{1} \\ (y_{2a}^L)^2 + M \cdot \mathbf{1} \\ -(y_{2a}^U \cdot y_{2a}^L) + M \cdot \mathbf{1} \\ (y_{1b}^L)^2 + M \cdot \mathbf{1} \\ (y_{1b}^U)^2 + M \cdot \mathbf{1} \\ (y_{1b}^L)^2 + M \cdot \mathbf{1} \\ -(y_{1b}^U \cdot y_{1b}^L) + M \cdot \mathbf{1} \\ (y_{2b}^L)^2 + M \cdot \mathbf{1} \\ (y_{2b}^U)^2 + M \cdot \mathbf{1} \\ (y_{2b}^L)^2 + M \cdot \mathbf{1} \\ -(y_{2b}^U \cdot y_{2b}^L) + M \cdot \mathbf{1} \\ \mathbf{0} \\ \mathbf{1} \end{pmatrix}.$$

Here, the number of decision variables is increased from n to $7n$ due to the inclusion of auxiliary variables y_1, y_2, w_1, w_2, q_a and q_b alongside the original decision variables x .

3.3.2 Epsilon Constraints

In this section, we just present the case for a single layer McCormick relaxation. It can be easily observed that this can be generalized to more layers just like the case of adaptive weights without loss of generality. The related ε -constraints in f_2 and f_1 can be respectively expressed as follows.

$$e^T w_2 + \text{lin}_2^T x \leq l_2 + \varepsilon \cdot (u_2 - l_2), \quad e^T w_1 + \text{lin}_1^T x \leq l_1 + \varepsilon \cdot (u_1 - l_1) \quad (17)$$

By relaxing $w_{2,i} = y_{2,i}^2 \quad \forall i = 1, \dots, n$ using a single-layer McCormick relaxation, the optimization problem in constraining f_2 can be expressed as follows.

$$\begin{aligned}
& \min_x f_1(x) \\
& \text{subject to: } Ax \leq b, \quad x_b \in \{0, 1\}^{2IT}, \quad x_L \leq x \leq x_U, & \text{(original constraints)} \\
& e^T w_2 + \text{lin}_2^T x \leq l_2 + \varepsilon \cdot (u_2 - l_2), \\
& w_2 \geq 2y_2 y_2^L - (y_2^L)^2, \\
& w_2 \geq 2y_2 y_2^U - (y_2^U)^2, \\
& w_2 \leq y_2(y_2^L + y_2^U) - y_2^U y_2^L, \\
& y_2 = L_2^T x.
\end{aligned}$$

Similarly, the new set of constraints $A_\varepsilon \cdot x \leq b_\varepsilon$ can be defined as follows.

$$A_\varepsilon = \begin{pmatrix} A & \mathbf{0} & \mathbf{0} \\ \text{lin}_2^T & \mathbf{0} & \mathbf{1} \\ \mathbf{0} & 2 \cdot \text{diag}(y_2^L) & -\mathbf{I} \\ \mathbf{0} & 2 \cdot \text{diag}(y_2^U) & -\mathbf{I} \\ \mathbf{0} & \text{diag}(-(y_2^U + y_2^L)) & \mathbf{I} \\ L_2^T & -\mathbf{I} & \mathbf{0} \end{pmatrix}, \quad b_\varepsilon = \begin{pmatrix} b \\ l_2 + \varepsilon(u_2 - l_2) \\ y_2^L \cdot y_2^L \\ y_2^U \cdot y_2^U \\ -(y_2^U \cdot y_2^L) \\ \mathbf{0} \end{pmatrix}.$$

Here, the number of decision variables increases from n to $3n$ due to the inclusion of auxiliary variables y_2 and w_2 alongside the original decision variables x . The procedure follows analogously for constraining objective f_1 .

4 Numerics

This section presents a comprehensive exploration of optimization techniques applied to the Multi-Objective Unit Commitment (MOUC) problem, focusing on methods that use realistic data for both thermal and hydroelectric units. The techniques evaluated include the Adaptive Weighted Sum (AWS) method and the ε -constraints approach, with a comparison of Gurobi's quadratic constraint handling and McCormick relaxation techniques. We start by outlining the data sources that were deployed. Next, we discuss the implementation of both uniform and adaptive weights for solving the unit commitment problem. Lastly, we investigate the impact of varying ε -constraints on the optimization results. By modifying the bounds of these constraints, we assess how these changes influence the optimal solutions, providing insight into the behavior of the objective functions under different constraint conditions. Hypervolume indicators are used to compare the quality of the Pareto fronts generated by each method. For further specifics on the implementation details, please check the gitHub repository¹.

4.1 Data Sources and Overview

For our study, we utilized data from two widely recognized sources [1,51]. The first dataset addresses the ramp-constrained hydro-thermal Unit Commitment problem [1], while the second, sourced from [51], focuses on emissions in the context of low-carbon MOUC. We integrate these datasets into a multiobjective optimization model that simultaneously considers economic cost, CO2 emissions, and sulfur emissions. This approach enables us to evaluate the environmental impact of different power generation schedules and identify strategies that balance emission reduction with economic efficiency. The details of both datasets are provided below for completeness.

4.1.1 Hydro-thermal dataset

This dataset includes randomly generated instances that emulate realistic scenarios and has been utilized in several works to validate algorithmic approaches [16,19,20]. The dataset includes detailed information on thermal and hydro units, such as their characteristics, constraints, and operational parameters. Key data includes the planning horizon length (24 periods), the number of thermal units (20), the number of hydro units (10), and a time-series of power demand values (loads) for each interval.

Thermal Units: Each thermal unit is defined by a unique identifier, cost coefficients (quadratic, linear, and constant), power output limits, minimum up-times and down-times, and start-up cost parameters, including cold and hot start-up costs, a time constant, maximum start-up time, and a fixed start-up cost.

¹Available at: <https://scm.cms.hu-berlin.de/aswinkannan1987/unitcommitment-springer-or>

Hydro Unit Description: Each hydro unit is defined by a unique identifier, a volume-to-power conversion coefficient, and minimum and maximum flood levels in the basin. The power output of the unit is directly related to the available water volume, which is determined by the flood levels. The maximum power output is calculated by multiplying the conversion coefficient by the maximum flood level, while the minimum power output is determined similarly using the minimum flood level. These calculations ensure that the hydro unit’s power output is proportional to the water available for conversion. Together, these parameters establish the operational power range of each hydro unit. These relationships can be mathematically expressed as follows:

$$\text{maxPower} = \text{scalingFactor} \cdot \text{volumeToPower} \cdot \text{maxFlood}$$

$$\text{minPower} = \text{scalingFactor} \cdot \text{volumeToPower} \cdot \text{minFlood}$$

To accurately reflect the power generation limits, the available water resources are used in the hydro units’ power output calculations. To prevent excessive reliance on hydro units, a scaling factor less than one is applied, reducing their maximum power output in the optimization model. This adjustment accounts for the economic advantage of hydro energy, given the assumption that it incurs no production costs, and helps balance other operational constraints and objectives.

4.1.2 Emissions Data

The emissions data in the model includes CO2 and sulfur emission coefficients, which are used to calculate emissions based on each unit’s power output. These coefficients are derived from established references and represent typical emission rates for different types of power plants. The sulfur emission coefficients are particularly useful for understanding the trade-offs between economic and operational decisions within the power sector.

In our model, we assumed that hydro units produce zero emissions, reflecting their characterization as a clean energy source. This assumption emphasizes the environmental benefits of hydroelectric power in our unit commitment analysis. We adapted emission coefficients originally designed for 10 thermal units, replicating them for the 20 thermal units in our study. For the sake of clarity, we note that the ideal penetration of hydro power would be 100 percent if they are not constrained by capacity. This limitation forces the presence of thermal units, which further imposes the regular constraints discussed above in addition to emissions cost.

Important: In our study throughout (including tabulations and figures), we note that the generation cost is measured in dollars and the emission levels are quantified by Metric Tonnes.

Optimization with Gurobi: All results presented in this study were computed using the Gurobi optimization solver, with a Matlab-based environment (R2023b) for model formulation. All the computation discussed in this section was performed on a MacAir Machine with a dualcore processor, with a speed of 1.6 GhZ and 8 GB of memory (RAM). The Matlab interface supports quadratic objectives, linear and quadratic inequality constraints, linear equalities, bound constraints, and special ordered set constraints (SOCs). Gurobi facilitates the management of multiple competing objectives, offering two key approaches for handling trade-offs as follows.

- **Blended Approach:** Optimizes a weighted combination of individual objectives.
- **Hierarchical (Lexicographic) Approach:** Prioritizes objectives and optimizes in order of priority, ensuring higher-priority objectives are not degraded.

In the context of optimization, quadratic constraints are essential for accurately representing problems that involve quadratic terms in their constraints. Gurobi provides a feature called `QuadCon` to handle these quadratic constraints effectively.

4.2 Uniform Weights

This section explains the use of the uniform weights method to solve a multiobjective unit commitment problem. In our case, since we consider just two objectives, the process of constructing the weight set is fairly straightforward. This takes the following form.

$$w_1^i = \frac{i}{n}, \quad w_2^i = 1 - w_1^i.$$

The study examined the impact of varying the number of weight pairs on the objective values in a multiobjective unit commitment problem with 2160 decision variables. The results for 10 different uniformly distributed weight pairs are presented in Table 1. The weight pairs (1,0) and (0,1) correspond

Weight Pair	Objective 1	Objective 2
(0.000, 1.000)	3306171.511	11.921
(0.111, 0.889)	2834788.460	121.099
(0.222, 0.778)	2834788.460	121.099
(0.333, 0.667)	2834788.460	121.099
(0.444, 0.556)	2834788.460	121.099
(0.556, 0.444)	2834788.460	121.099
(0.667, 0.333)	2834788.460	121.099
(0.778, 0.222)	2834788.460	121.099
(0.889, 0.111)	2834788.460	121.099
(1.000, 0.000)	2834788.460	121.099

Table 1: Objective values for $n = 2160$ and each uniform weight pair

to single-objective optimizations for objectives f_1 and f_2 respectively, showing the minimum cost and emissions under constraints. The pair (0,1) produced notably different results, with objective values of 3306171.511 for cost and 11.921 for emissions, compared to the other weight pairs, which yielded values of 2834788.460 for cost and 121.099 for emissions. This difference underscores the importance of further exploring the Pareto front between these extremes to better understand the trade-offs and potential benefits of intermediate weight pairs. The performance of the uniform weights method was evaluated in the multiobjective unit commitment problem by testing it with different numbers of decision variables and weight pairs, while documenting the runtimes for each configuration. The number of decision variables was varied by changing the number of time steps. The results are summarized in Tables 2 and 3. The total runtime includes the time spent on data processing, cost calculations, constructing constraint and objective matrices, and solving the model with Gurobi for each weight pair. The Gurobi runtime specifically refers to the time spent on solving the optimization problem with Gurobi.

n	nr. of pairs					
	10	20	30	40	50	60
2160	7.55	13.58	20.54	25.60	33.33	39.29
4320	20.84	29.02	37.39	43.24	50.88	59.00
6480	58.41	71.49	75.72	85.57	99.22	105.73
8640	144.47	150.60	163.94	172.44	184.53	193.76
10800	264.68	296.26	306.82	327.89	375.07	382.80

Table 2: Total Runtimes (s) for various numbers of decision variables and uniform weight pairs

n	nr. of pairs					
	10	20	30	40	50	60
2160	5.58	11.62	17.96	23.61	31.32	36.70
4320	7.44	15.23	23.99	32.05	39.73	48.32
6480	9.84	18.63	28.75	38.04	48.69	57.29
8640	12.09	23.32	33.31	44.08	58.06	72.45
10800	19.37	39.08	57.60	74.90	99.98	119.53

Table 3: Gurobi Runtimes (s) for various numbers of decision variables and uniform weight pairs

The total runtime and Gurobi runtime for various configurations of decision variables and weight pairs show distinct behaviours. As expected, both the total runtime and the Gurobi runtime increase with the number of decision variables and the number of weight pairs. Figure 4 illustrates the total runtimes and Gurobi runtimes for 10 weight pairs. The computational time appears to scale polynomially. This growth in total runtime is primarily due to the presence of increasing overheads as the number of decision variables grows, apart from the optimization time. The Gurobi runtime, which measures the time spent solely on solving the optimization problem, also shows an increase with more decision variables and weight pairs. However, while the problem size increases, it constitutes smaller proportions of the total runtime compared to other tasks such as data handling and matrix construction.

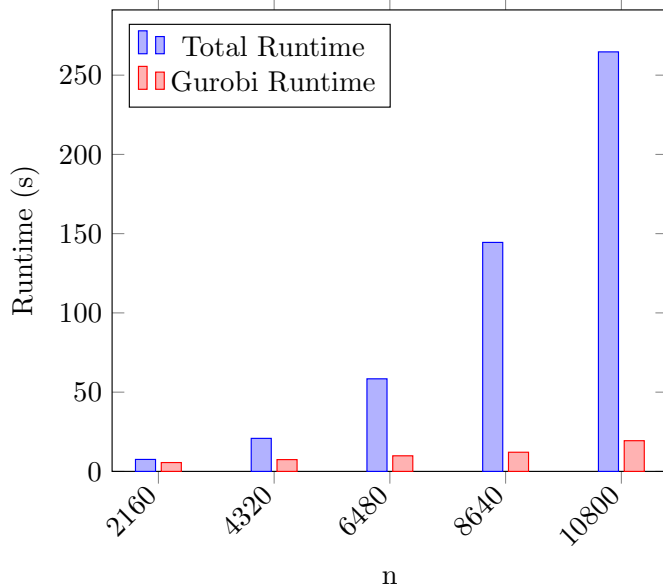


Figure 4: Total and Gurobi Runtimes for 10 weight pairs

4.3 Adaptive Weights

This section covers the application of our proposed method of adaptive weights, in combination with McCormick relaxations. The computational performance of the adaptive methods is compared against Gurobi’s `QuadCon` and that of weighted methods.

4.3.1 Formulation

The adaptive weights method begins with an initial weighted sum optimization to establish a baseline understanding of the objective trade-offs. This initial step uses $n_{\text{initial}} = 10$ uniformly distributed weight pairs, yielding the results in Table 4. After this initial optimization, we proceed through the steps

Solutions	Objective 1	Objective 2
P_1	3306171.511	11.921
P_2	2834788.460	121.099
P_3	2834788.460	121.099
P_4	2834788.460	121.099
P_5	2834788.460	121.099
P_6	2834788.460	121.099
P_7	2834788.460	121.099
P_8	2834788.460	121.099
P_9	2834788.460	121.099
P_{10}	2834788.460	121.099

Table 4: Objective values for $n = 2160$ and 10 uniform weight pairs

outlined in the previous section. The results in Table 5 show the total and Gurobi runtimes, along with the optimal values for f_1 and f_2 , obtained using the adaptive weights method for different values of decision variables n . As n increases (due to more time steps), both runtimes increase significantly, as expected. For example, at $n = 540$, the total runtime is 19.77 seconds, but at $n = 12960$, it rises to 2417.49 seconds. The adaptive weights method generally results in higher runtimes compared to the uniform weights method, due to the additional complexity of dynamically adjusting weights. However, for $n = 2160$, the adaptive method successfully explores the Pareto front between two points identified using the uniform weights method. The final Pareto points are stored for further analysis. The majority of the total runtime is spent on the Gurobi optimization process, particularly when using its `QuadCon` feature to handle quadratic constraints. The effectiveness of the adaptive weights method was evaluated

n	Total Runtime (s)	Gurobi Runtime (s)	Optimal f_1	Optimal f_2
540	19.77	19.37	717661.658	22.246
1080	30.02	29.44	1438587.163	41.824
1620	63.51	62.55	2157642.324	62.883
2160	70.00	68.61	2878614.292	82.412
2700	74.96	72.83	3599634.371	101.179
3240	77.19	73.81	4317964.333	123.545
3780	84.18	78.61	5037515.019	144.279
4320	172.57	167.66	5756169.879	166.199
4860	214.66	207.81	6478500.930	183.237
5400	317.09	308.21	7199182.782	202.468
5940	391.10	378.19	7918177.252	223.966
6480	466.04	479.77	8638558.918	243.593
7020	555.22	533.80	9359554.651	262.397
7560	706.52	684.14	10081211.717	280.347
8100	718.93	695.75	10801162.644	300.568
8640	908.87	885.74	11520305.713	321.839
9180	962.22	936.23	12237578.410	345.602
9720	1007.20	974.50	12952620.790	372.476
10260	1247.08	1212.62	13677457.939	386.039
10800	1571.24	1531.47	14399600.872	403.380
11340	1853.91	1803.21	15120516.449	422.196
11880	2095.26	2018.11	15837393.454	446.522
12420	2240.76	2176.19	16553431.198	471.962
12960	2417.49	2343.15	17267926.285	499.417

Table 5: Total and Gurobi Runtimes for Adaptive Weights using QuadCon

using the Hypervolume (HV) metric [2,4,50], computed with the PyGMO library². The HV was calculated from the non-dominated objective values obtained through the adaptive weights method using QuadCon. For each value of n (number of decision variables), the reference point was set to be approximately 1.2 worse than the worst objective function value across all solutions. The results, presented in Table 6, show that HV values increase as n increases. However, this increase in HV is not due to better Pareto solutions but because the objective space expands as n grows.

n	Pareto Points	Total (s)	Gurobi (s)	HV ($\cdot 10^7$)
540	6	19.77	19.37	0.22
1080	6	30.02	29.44	0.88
1620	6	63.51	62.55	1.99
2160	6	70.00	68.61	3.51
2700	6	74.96	72.83	5.56

Table 6: Hypervolume Indicator for Adaptive Weights for various numbers of decision variables using QuadCon

4.3.2 Quadratic Constraints with single-layer McCormick

For our next numerical experiment, we relax the quadratic constraints by using a single-layer McCormick relaxation. Table 7 presents the total runtime, Gurobi runtime, and optimized objective values for various numbers of decision variables using the single-layer McCormick relaxation. The number of decision variables presented in table 7 only accounts for the original decision variables x (and not the auxiliary variables introduced) and is varied by changing the number of time steps considered. The results in table 7 demonstrate that using the single-layer McCormick relaxation significantly reduces the runtime in comparison to using the primitive version of Quadcon and Gurobi. Notably, the computational time appears to scale polynomially as the problem size grows. Along with that, e.g. for $n = 2160$, we observe that the adaptive weights method using single-layer McCormick relaxation effectively explores the Pareto

²<https://readthedocs.org/projects/pygmo/downloads/pdf/newdocs/>

n	Total Runtime (s)	Gurobi Runtime (s)	Optimal f_1	Optimal f_2
540	7.59	6.87	735203.203	8.361
1080	8.48	7.36	1472770.926	15.530
1620	18.69	15.77	2204594.811	25.593
2160	19.26	15.86	2939702.566	34.002
2700	22.43	17.20	3674927.273	42.352
3240	27.54	20.41	4410151.981	50.702
3780	32.85	23.07	5145376.688	59.052
4320	38.88	24.54	5880601.472	67.401
4860	43.48	25.09	6615826.182	75.751
5400	51.96	28.34	7351050.874	84.101
5940	58.71	29.75	8086275.514	92.451
6480	66.52	31.29	8821500.273	100.800
7020	77.08	31.90	9556725.012	109.150
7560	93.23	40.56	10291949.721	117.500
8100	127.17	50.91	11027174.431	125.850
8640	135.06	61.70	11761157.401	134.826
9180	163.37	67.20	12497623.824	142.549
9720	195.49	73.70	13232028.710	151.313
10260	217.08	86.96	13968073.186	159.249
10800	255.97	95.01	14701927.560	168.290
11340	290.33	99.40	15437081.978	176.675
11880	327.06	114.55	16170873.284	185.060
12420	382.05	114.67	16908972.098	192.648
12960	412.56	133.63	17644196.814	200.998

Table 7: Total and Gurobi Runtimes for Adaptive Weights using single-layer McCormick

front between the points $P1$ (3306171.511, 11.921) and $P2$ (2834788.460, 121.099), identified using initial uniform weights method. Additionally, it can be noted that the **Gurobi** runtime constitutes a significant portion of the total runtime, though not as much as with using **QuadCon**. Similar to the previous section, we compute the HV metric using the **PyGMO** library. Table 8 provides the HV values for different values of n alongside the total and Gurobi runtimes, and the number of Pareto points. To ensure a fair comparison,

n	Pareto Points	Total (s)	Gurobi (s)	HV ($\cdot 10^7$)
540	6	7.59	6.87	0.23
1080	6	8.48	7.36	0.91
1620	6	18.69	15.77	2.05
2160	6	19.26	15.86	3.65
2700	6	22.43	17.20	5.75

Table 8: Hypervolume Indicator for Adaptive Weights for various numbers of decision variables using single-layer McCormick

we use the same reference points as in 6. Comparing the HV values between tables 6 and 8, we observe that the single-layer McCormick method generally yields higher HV values than the **QuadCon** method for the same values of n .

4.3.3 Quadratic Constraints with 2-layer McCormick

Next, the quadratic constraints were relaxed using a two-layer McCormick relaxation. Table 9 presents the total runtime, Gurobi runtime, and final Pareto points derived from this method for various numbers of decision variables using this approach. The 2-layer McCormick method results in higher runtimes than the 1-layer method due to the larger problem size, but its solutions are slightly closer to those achieved with **QuadCon**. Increasing the number of layers can improve the accuracy further. Despite introducing additional auxiliary variables in the 2-layer method, its runtime remains generally lower than that of **QuadCon**. Hypervolume (HV) values, presented in Table 10, show a similarly increasing trend with the number of decision variables n , comparable to the 1-layer McCormick method. This suggests that while

n	Total Runtime (s)	Gurobi Runtime (s)	Optimal f_1	Optimal f_2
540	19.14	18.06	734051.668	8.941
1080	25.36	23.57	1468676.718	17.593
1620	35.38	31.16	2202605.370	26.596
2160	44.21	36.73	2937180.436	35.274
2700	57.02	46.32	3671755.841	43.951
3240	67.92	50.45	4406330.843	52.628
3780	71.63	51.60	5140906.017	61.305
4320	175.75	143.93	5875481.108	69.983
4860	235.29	193.27	6610056.335	78.660
5400	255.28	201.73	7344631.358	87.337
5940	320.05	253.27	8079206.517	96.015
6480	478.27	393.82	8813796.018	104.685
7020	557.79	453.59	9548371.189	113.362
7560	643.21	502.27	10282946.309	122.039
8100	752.10	597.37	11017507.075	130.724
8640	796.29	622.05	11752082.178	139.401
9180	932.82	678.97	12486667.585	148.073
9720	1057.00	718.63	13221232.476	156.755
10260	1106.27	752.45	13955807.595	165.433
10800	1207.11	785.45	14690382.752	174.110
11340	1393.50	867.25	15424967.464	182.782
11880	1832.32	1179.51	16159533.023	191.464
12420	1946.83	1294.42	16894108.174	200.142
12960	2044.38	1364.24	17628698.231	208.811

Table 9: Total and Gurobi Runtimes for Adaptive Weights using 2-layer McCormick

the two-layer method adds complexity, its performance in exploring the objective space is similar to that of the one-layer method.

n	Pareto Points	Total (s)	Gurobi (s)	HV ($\cdot 10^7$)
540	6	19.14	18.06	0.23
1080	6	25.36	23.57	0.91
1620	6	35.38	31.16	2.05
2160	6	44.21	36.73	3.65
2700	6	57.02	46.32	5.75

Table 10: Hypervolume Indicator for Adaptive Weights for various numbers of decision variables using 2-layer McCormick

4.3.4 QuadCon vs. single- and multi-layer McCormick

Table 11 and Figure 5 compare the Gurobi runtimes for the adaptive weights method across different values of n for three distinct approaches to handling quadratic constraints: **QuadCon**, single-layer McCormick, and 2-layer McCormick relaxations. The results in Table 11 reveal that the single-layer McCormick relaxation consistently achieves the lowest runtime across all values of n , demonstrating its efficiency and applicability to large scale optimization problems. In contrast, the **QuadCon** method, which directly handles quadratic constraints, has the highest runtime, especially as the number of decision variables increases. This method’s computational intensity is evident from the increase in runtime as n grows, reaching over 2300 seconds for $n = 12960$. The 2-layer McCormick relaxation, while not as fast as the single-layer approach, still offers a considerable improvement over the **QuadCon** method, thereby finding a balance. For completeness, Figure 5 illustrates the runtime trends for each method as n increases.

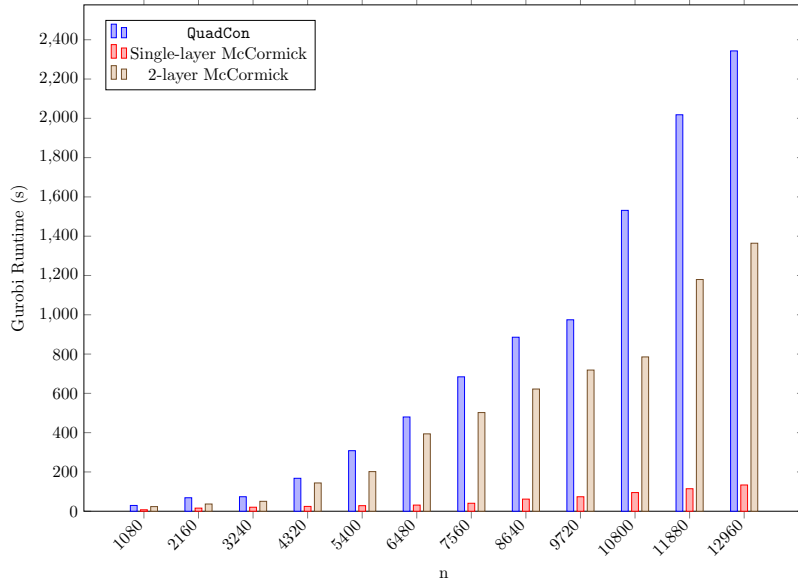


Figure 5: Comparison of Gurobi Runtimes for Adaptive Weights using **QuadCon**, 1-layer and 2-layer McCormick

Overhead: To assess the efficiency of the methods in handling quadratic constraints, both the Gurobi solve time and the additional overhead from auxiliary variables and constraints must be considered. Table 12 and Figure 6 present the total runtimes for the **QuadCon**, single-layer McCormick, and 2-layer McCormick methods across various values of n . The total runtime analysis shows that the single-layer McCormick method is the fastest overall, with lower total runtimes compared to the 2-layer McCormick and **QuadCon** methods, especially for larger problem sizes. Although the Gurobi solve times for the McCormick methods are faster, their overhead from extra auxiliary variables and larger matrices reduces the performance gains. Future work could focus on optimizing this overhead to improve computational efficiency.

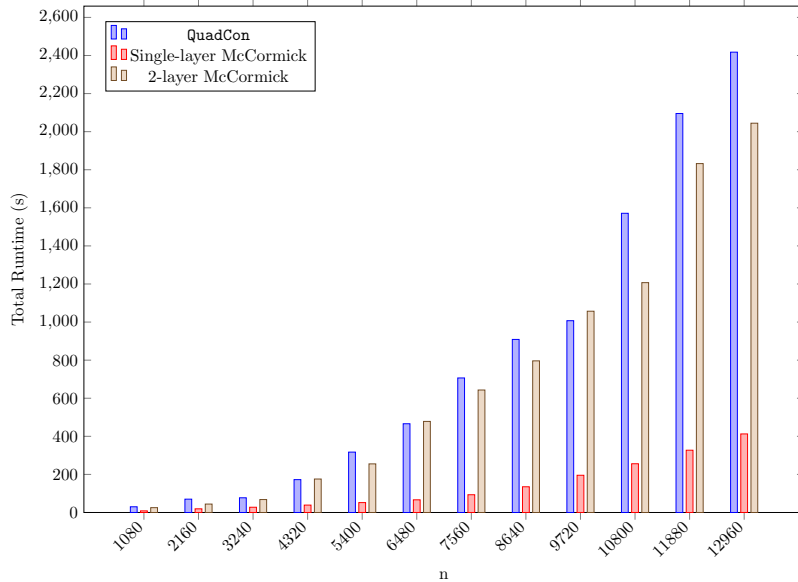


Figure 6: Comparison of Total Runtimes for Adaptive Weights using **QuadCon**, 1-layer and 2-layer McCormick

The runtime for the **QuadCon** method initially increases polynomially, but at higher n values, it begins to show signs of exponential growth, highlighting the computational challenges of handling quadratic constraints in higher dimensions. To assess solution quality, the Hypervolume (HV) Indicator is used, with comparisons for different methods presented in Table 13, using the same reference point for each n . The

n	QuadCon (s)	Single-layer McCormick (s)	2-layer McCormick (s)
540	19.37	6.87	18.06
1080	29.44	7.36	23.57
1620	62.55	15.77	31.16
2160	68.61	15.86	36.73
2700	72.83	17.20	46.32
3240	73.81	20.41	50.45
3780	78.61	23.07	51.60
4320	167.66	24.54	143.93
4860	207.81	25.09	193.27
5400	308.21	28.34	201.73
5940	378.19	29.75	253.27
6480	479.77	31.29	393.82
7020	533.80	31.90	453.59
7560	684.14	40.56	502.27
8100	695.75	50.91	597.37
8640	885.74	61.70	622.05
9180	936.23	67.20	678.97
9720	974.50	73.70	718.63
10260	1212.62	86.96	752.45
10800	1531.47	95.01	785.45
11340	1803.21	99.40	867.25
11880	2018.11	114.55	1179.51
12420	2176.19	114.67	1294.42
12960	2343.15	133.63	1364.24

Table 11: Comparison of Gurobi Runtimes for Adaptive Weights using QuadCon, 1-layer and 2-layer McCormick

n	QuadCon (s)	Single-layer McCormick (s)	2-layer McCormick (s)
540	19.77	7.59	19.14
1080	30.02	8.48	25.36
1620	63.51	18.69	35.38
2160	70.00	19.26	44.21
2700	74.96	22.43	57.02
3240	77.19	27.54	67.92
3780	84.18	32.85	71.63
4320	172.57	38.88	175.75
4860	214.66	43.48	235.29
5400	317.09	51.96	255.28
5940	391.10	58.71	320.05
6480	466.04	66.52	478.27
7020	555.22	77.08	557.79
7560	706.52	93.23	643.21
8100	718.93	127.17	752.10
8640	908.87	135.06	796.29
9180	962.22	163.37	932.82
9720	1007.20	195.49	1057.00
10260	1247.08	217.08	1106.27
10800	1571.24	255.97	1207.11
11340	1853.91	290.33	1393.50
11880	2095.26	327.06	1832.32
12420	2240.76	382.05	1946.83
12960	2417.49	412.56	2044.38

Table 12: Comparison of Total Runtimes for Adaptive Weights using QuadCon, 1-layer and 2-layer McCormick

n	Pareto Points	HV (Q) ($\cdot 10^7$)	HV (1-l. M) ($\cdot 10^7$)	HV (2-l. M) ($\cdot 10^7$)
540	6	0.22	0.23	0.23
1080	6	0.88	0.91	0.91
1620	6	1.99	2.05	2.05
2160	6	3.51	3.65	3.65
2700	6	5.56	5.75	5.75

Table 13: Comparison of Hypervolume Indicator for Adaptive Weights using QuadCon, 1-layer McCormick, and 2-layer McCormick methods

McCormick relaxation methods (single-layer and 2-layer) reduce computational burden without compromising the quality of Pareto solutions compared to QuadCon. The slight differences in Hypervolume (HV) values are due to the broader exploration of the Pareto front enabled by relaxing quadratic constraints, allowing for a larger search space. Overall, the McCormick methods offer a significant improvement in runtime while maintaining similar solution quality to QuadCon, with the single-layer McCormick method being the most efficient for the MOUC problem, balancing both efficiency and solution quality.

4.4 Epsilon Constraints

In this section, we explore the epsilon constraints method for solving our biobjective problem of interest. As earlier, we focus on both versions, i.e. Quadcon and McCormick relaxations.

4.4.1 Quadratic Constraints with QuadCon

First, we discuss the process of optimization using varying ε for the quadratic constraints using Gurobi’s QuadCon functionality. The corresponding formulation has been discussed in the previous section. As earlier, we vary the problem dimension n and record the performance of Gurobi and Quadcon. For $n = 2160$, Table 14 presents the results of optimizing the first objective function, f_1 , while treating the second objective function f_2 as a constraint, with varying ε values. The upper bound for f_2 increases incrementally with the values of ε (from 0 to 1).

ε	Upper Bound for f_2	Optimal $f_1(x)$
0.0	$f_2(x) \leq 12.544$	3080916.175
0.1	$f_2(x) \leq 23.400$	2977178.832
0.2	$f_2(x) \leq 34.255$	2940355.755
0.3	$f_2(x) \leq 45.111$	2918969.545
0.4	$f_2(x) \leq 55.966$	2898231.487
0.5	$f_2(x) \leq 66.822$	2884766.524
0.6	$f_2(x) \leq 77.677$	2871860.374
0.7	$f_2(x) \leq 88.533$	2860818.942
0.8	$f_2(x) \leq 99.388$	2851375.563
0.9	$f_2(x) \leq 110.244$	2843023.920
1.0	$f_2(x) \leq 121.099$	2835606.661

Table 14: Results for ε -constraints using QuadCon

Tables 15 and 16 provide an overview of the total runtime and the Gurobi runtime, respectively, for increasing ε values from 0 to 1, and increasing dimensionality (n). From Tables 15 and 16, we observe that the total and Gurobi runtimes increase with the number of decision variables and the decrease in step sizes. For smaller n (say, $n = 2160$), the difference between the total runtime and Gurobi runtime is relatively small. This indicates that a significant portion of the runtime is spent on actual optimization. However, as the number of decision variables increases (e.g., 10800), the proportion of total runtime to Gurobi runtime increases in proportion. This difference can be attributed to the overhead of data pre-processing and construction of objective and constraint matrices, which become substantial as the problem size grows. Table 17 provides the Hypervolume (HV) Indicator values for $n = 2160$ and different step sizes in the ε -constraints method for f_1 using QuadCon. The number of Pareto points obtained for each step size is also indicated in table 17. The number of Pareto points and the Hypervolume (HV) values increase as step sizes decrease, due to finer granularity that allows for a more detailed exploration

n \ Step Size	0.2	0.1	0.05	0.025	0.0125
1080	4.52	9.61	17.83	33.3	69.43
2160	7.41	15.77	30.85	56.66	111.94
3240	10.75	26.79	49.31	90.78	162.42
4320	35.42	63.84	116.8	180.44	307.76
5400	48.49	84.96	146.7	252.59	443.45
6480	75.04	122.37	180.1	290.77	545.1
7560	115.76	166.78	243.61	414.27	697.38
8640	145.07	240.78	349.66	464.79	888.99
9720	228.25	334.45	417.19	591.14	1088.37
10800	314.4	401.66	501.33	687.98	1228.2

Table 15: Total Runtime (s) for ε -constraints using QuadCon with objective f_1 and constraining f_2

n \ Step Size	0.2	0.1	0.05	0.025	0.0125
1080	3.71	8.73	16.92	32.08	67.57
2160	5.48	13.96	29.08	54.66	109.22
3240	6.44	22.21	44.4	85.12	155.06
4320	22.57	53.28	105.92	169.18	296.53
5400	23.07	61.43	122.93	230.42	418.48
6480	25.48	66.81	129.74	241.04	496.05
7560	26.77	90.03	170.84	335.35	612.15
8640	29.88	115.33	218.1	342.95	762.71
9720	57.36	140.43	241.4	422.32	925.16
10800	64.05	167.65	248.98	439.03	975.69

Table 16: Gurobi Runtime (s) for ε -constraints using QuadCon with objective f_1 and constraining f_2

Step Size	Total (s)	Gurobi (s)	Pareto Points	HV ($\cdot 10^7$)
0.2	7.41	5.48	6	4.29
0.1	15.77	13.96	11	4.46
0.05	30.85	29.08	21	4.54
0.025	56.66	54.66	41	4.58
0.0125	111.94	109.22	81	4.60

Table 17: Hypervolume Indicator for ε -constraints using QuadCon with objective f_1 and constraining f_2

of the Pareto front. This leads to a better representation of the Pareto front, although it also requires more computational effort. Additionally, the study also examined the optimization of f_2 with a constraint on f_1 . The total and Gurobi runtime for different step sizes and numbers of decision variables are shown in Tables 18 and 19, respectively. The runtime trends for optimizing f_2 follow a similar pattern to those for f_1 , with both total runtime and Gurobi runtime increasing as the number of decision variables and the step size decrease. However, the increase in runtime is more pronounced for f_2 , especially for larger values of n . For example, the total runtime exceeds 12,822 seconds for $n = 9720$ and step size 0.2, and surpasses 20,000 seconds for smaller step sizes and larger n . Additionally, the proportion of Gurobi runtime within the total runtime is higher when optimizing f_2 , indicating that a significant portion of the time is spent on solving the optimization problem using Gurobi. The longer runtime for f_2 is attributed to the increased computational complexity of constraining f_1 , which results in more complex constraints and a larger objective space. Table 20 presents the Hypervolume (HV) values for the ε -constraints method when optimizing f_2 using QuadCon, across various step sizes. Similar to the results for f_1 , the number of distinct Pareto points increases with smaller step sizes, as finer granularity allows for more detailed exploration and a higher number of optimization runs. This leads to an increase in HV values and an enhanced Pareto frontier.

n \ Step Size	Step Size				
	0.2	0.1	0.05	0.025	0.0125
1080	12.06	20.12	28.76	64.57	130.56
2160	19.22	33.36	57.72	141.72	268.95
3240	77.99	94.41	204.25	388.61	719.98
4320	141.28	169.26	414.99	753.04	1603.93
5400	315.77	375.54	956.30	1909.03	3691.47
6480	808.99	918.20	3386.30	5680.24	10752.95
7560	1501.76	1685.81	7416.45	15472.55	*
8640	3287.61	3531.25	18339.38	*	*
9720	12822.71	13182.87	*	*	*
10800	*	*	*	*	*

Table 18: Total Runtime (s) for ε -constraints using QuadCon with objective f_2 and constraining f_1

n \ Step Size	Step Size				
	0.2	0.1	0.05	0.025	0.0125
1080	10.48	19.32	27.87	63.38	128.91
2160	17.33	30.98	55.30	139.10	266.12
3240	72.29	89.37	199.89	383.75	712.82
4320	130.52	159.04	403.29	741.02	1591.85
5400	290.62	352.39	933.15	1884.49	3666.34
6480	760.29	875.91	3344.42	5632.03	10693.24
7560	1423.18	1619.74	7349.72	15402.42	*
8640	3185.15	3425.45	18237.44	*	*
9720	12664.94	13042.98	*	*	*
10800	*	*	*	*	*

Table 19: Gurobi Runtime (s) for ε -constraints using QuadCon with objective f_2 and constraining f_1

Step Size	Total (s)	Gurobi (s)	Pareto Points	HV ($\cdot 10^7$)
0.2	19.22	17.33	6	2.43
0.1	33.36	30.98	11	2.58
0.05	57.72	55.30	21	2.66
0.025	141.72	139.10	41	2.69
0.0125	268.95	266.12	81	2.71

Table 20: Hypervolume Indicator for ε -constraints using QuadCon with objective f_2 and constraining f_1

4.4.2 Quadratic Constraints with McCormick

With the introduction of McCormick relaxations, the number of decision variables is seen to increase from n to $3n$. Note that this is due to the introduction of auxiliary variables y_2 and w_2 . For $n = 2160$, optimization results for the objective f_1 using McCormick relaxations are presented in Table 21. The table shows both the upper bounds and actual values of f_2 for varying ε values along with the optimal values of f_1 . The results highlight that McCormick relaxation sometimes leads to deviations from the upper bound for f_2 , which is expected. Adjustments to the bounds are made to ensure feasibility and to avoid generating identical solutions. As seen in the results with QuadCon in Table 14, as ε increases from 0.0 to 1.0, the optimal value of f_1 decreases, suggesting that relaxing the constraint in f_2 allows for a more favorable optimization of f_1 . Similarly, both the upper bound and actual value of f_2 increase as ε increases, reflecting the relaxation of the constraint on f_2 .

ε	Upper Bound for $f_2(x)$	$f_2(x)$	Optimal $f_1(x)$
0.0	12.544	13.147	3070051.332
0.1	23.508	24.085	2974187.435
0.2	34.472	35.069	2938771.839
0.3	45.435	46.089	2917024.659
0.4	56.399	57.143	2896820.000
0.5	67.363	68.126	2883210.770
0.6	78.327	79.197	2870070.570
0.7	89.290	90.178	2859408.273
0.8	100.254	101.182	2849989.210
0.9	111.218	112.233	2841494.910
1.0	122.182	122.182	2834788.460

Table 21: Results for objective f_1 and ε -constraints on f_2 using McCormick

Tables 22 and 23 present the total and Gurobi runtime, respectively, for varying n and step sizes using the single-layer McCormick relaxation. The number of decision variables presented only accounts for the original decision variables x .

n \ Step Size	0.2	0.1	0.05	0.025	0.0125
1080	4.67	9.2	17.41	35.03	70.64
2160	9.01	14.75	25.13	45.57	85.11
3240	12.83	22.35	36.03	62.21	123.16
4320	19.95	35.5	53.05	83.83	142.29
5400	32.31	49.08	70.49	112.26	191.23
6480	47.2	61.64	99.77	147.93	247.26
7560	78.43	98.27	149.09	198.01	335.08
8640	92.67	123.13	165.25	259.01	389.19
9720	119.39	168.26	231.31	317.09	464.33
10800	144.59	193.57	254.91	370.33	589.4

Table 22: Total Runtime (s) for objective f_1 and ε -constraints on f_2 using McCormick

n \ Step Size	0.2	0.1	0.05	0.025	0.0125
1080	3.84	8.17	16.27	33.87	68.67
2160	5.67	12.16	22.54	42.79	81.99
3240	5.83	15.54	29.81	55.08	109.8
4320	6.02	22.03	39.58	69.43	128.36
5400	9.39	26.02	45.61	83.79	167.55
6480	11.12	27.47	65.61	113.47	210.19
7560	13.26	37.36	93.12	143.08	281.36
8640	16.88	47.98	93.76	185.1	316.61
9720	18.77	57.21	120.53	219.87	364.02
10800	14.24	62.49	130.73	236.99	458.01

Table 23: Gurobi Runtime (s) for objective f_1 and ε -constraints on f_2 using McCormick

As expected, we observe that both the total and Gurobi runtimes increase with the number of decision variables and the decrease in step sizes. Comparing these results with those obtained using **QuadCon**, we see that the McCormick relaxation method improves the runtime performance, particularly with larger problem dimension. The reduction in runtime can be attributed to the relaxation of quadratic constraints into linear constraints, which are computationally less intensive for the solver to handle, despite the addition of auxiliary variables. Table 24 provides the Hypervolume (HV) Indicator values and the number of Pareto points for $n = 2160$ using different step sizes in the ε -constraints method for f_1 with **QuadCon**. As expected, while smaller step sizes require more computational effort, they yield

more Pareto points and higher HV values, indicating an improved quality of the Pareto front. Similarly,

Step Size	Total (s)	Gurobi (s)	Pareto Points	HV ($\cdot 10^7$)
0.2	9.01	5.67	6	4.29
0.1	14.75	12.16	11	4.46
0.05	25.13	22.54	21	4.54
0.025	45.57	42.79	41	4.58
0.0125	85.11	81.99	81	4.60

Table 24: Hypervolume Indicator for ε -constraints for minimizing f_1 and constraining f_2 using McCormick

tables 25 and 26 provide an overview of the total runtime and the Gurobi runtime, respectively, for different step sizes and increasing numbers of decision variables for optimizing f_2 and constraining f_1 using the McCormick relaxation method. The comparative statistics between **Quadcon** and McCormick

n \ Step Size	0.2	0.1	0.05	0.025	0.0125
1080	3.91	7.68	13.34	26.29	56.18
2160	7.5	13.68	18.86	35.98	73.51
3240	16.05	21.33	31.41	53.42	94.95
4320	20.87	30.03	40.85	64.88	113.12
5400	32.85	40.51	55.09	83.68	137.94
6480	44.55	54.14	67.45	110.31	181.16
7560	67.02	79.04	94.29	122.47	201.13
8640	89.63	112.57	126.41	154.58	257.86
9720	116.9	132.33	144.78	186.97	293.91
10800	151.68	163.44	187	219.19	330.87

Table 25: Total Runtime (s) for minimizing f_2 and constraining f_1 using McCormick

n \ Step Size	0.2	0.1	0.05	0.025	0.0125
1080	3.03	6.72	12.14	25.39	54.94
2160	4.51	10.14	15.97	32.77	69.7
3240	6.1	13.11	22.99	45.14	87.32
4320	6.64	14.96	26.23	51.07	98.01
5400	6.22	15.52	27.47	56.81	112.38
6480	7.07	16.27	29.72	60.76	140.48
7560	10.82	21.38	35.79	66.7	146.63
8640	10.39	25.56	40.35	76.18	183.45
9720	12.57	29.48	42.58	85.65	197.26
10800	12.74	30.92	50.67	89.88	204.72

Table 26: Gurobi Runtime (s) for minimizing f_2 and constraining f_1 using McCormick

relaxations are similar here as well, where a significant reduction in the computational effort with the latter. For instance, with $n = 10800$ and a step size of 0.2, Gurobi solved the problem in 12.74 seconds using the McCormick relaxation, whereas with **QuadCon**, it exceeded 20,000 seconds. Additionally, the total runtime with McCormick, including overhead, is 151.68 seconds, demonstrating the efficiency of the McCormick approach despite the additional auxiliary variables.

4.4.3 QuadCon vs. McCormick

Figure 7 displays the total runtimes for the **QuadCon** and single-layer McCormick methods across various values of n . Note that in this case, f_1 is minimized and f_2 is constrained. These results further confirm that the single-layer McCormick method consistently demonstrates lower total runtimes, making it the faster approach for handling quadratic constraints compared to **QuadCon** in our optimization problem.

Step Size	Total (s)	Gurobi (s)	Pareto Points	HV ($\cdot 10^7$)
0.2	7.50	4.51	6	2.43
0.1	13.68	10.14	11	2.55
0.05	18.86	15.97	21	2.59
0.025	35.98	32.77	41	2.62
0.0125	73.51	69.70	81	2.63

Table 27: Hypervolume Indicator for ε -constraints for minimizing f_2 and constraining f_1 using McCormick

Table 28 compares the performance of the QuadCon and McCormick methods in the ε -constraints method

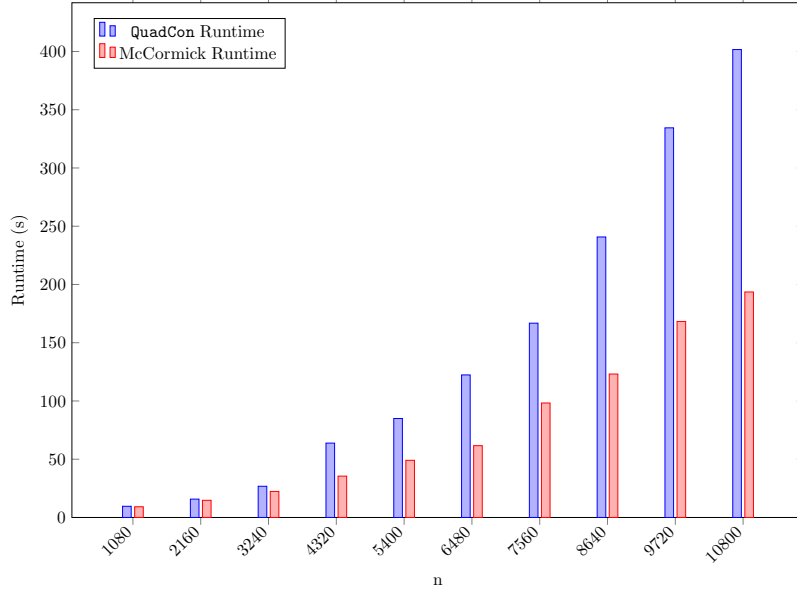


Figure 7: Comparison of Total Runtimes for ε -constraints using QuadCon vs. McCormick with Step Size 0.1 for optimizing f_1 and constraining f_2

for minimizing f_1 (and constraining f_2), presenting the number of Pareto points, Gurobi runtimes, and HV values calculated by using the same reference points for different step sizes. Despite the differences in runtimes, the McCormick relaxation method does not compromise on the quality of the Pareto solutions. This is reflected in the HV values, which remain consistently high and closely match those obtained with QuadCon. Table 29 compares the total runtimes for solving the optimization problem with objective f_2

Step Size	Pareto Points	Runtime (Q)	Runtime (M)	HV (Q)	HV (M)
0.2	6	5.48	5.67	4.29	4.29
0.1	11	13.96	12.16	4.46	4.45
0.05	21	29.08	22.54	4.54	4.53
0.025	41	54.66	42.79	4.58	4.57
0.0125	81	109.22	81.99	4.60	4.59

Table 28: Comparison of Hypervolume Indicator for ε -constraints using QuadCon vs. McCormick for minimizing f_1 and constraining f_2

(and constraining f_1) using the ε -constraints method with QuadCon and McCormick relaxations. The analysis shows that, similar to f_1 , McCormick relaxation outperforms QuadCon, with differences becoming even more significant for f_2 . Specifically, the complexity of the QuadCon method grows exponentially as the number of decision variables increases. For larger values of n (greater than 9720), QuadCon runtimes exceed 20,000 seconds, while McCormick relaxation allows the problem to be solved in just 163.44 seconds. Table 30 compares the efficiency of QuadCon and McCormick in the ε -constraints method for minimizing f_2 (and constraining f_1), presenting the number of Pareto points, Gurobi runtimes, and HV

n	QuadCon Runtime(s)	McCormick Runtime(s)
1080	20.12	7.68
2160	33.36	13.68
3240	94.41	21.33
4320	169.26	30.03
5400	375.54	40.51
6480	918.20	54.14
7560	1685.81	79.04
8640	3531.25	112.57
9720	13182.87	132.33
10800	*	163.44

Table 29: Comparison of Total Runtimes for ε -constraints using QuadCon vs. McCormick with Step Size 0.1 for minimizing f_2 and constraining f_1

values for different step sizes using the same reference points. Although the runtimes differ significantly between the two methods, the HV values are similar. The difference in HV is due to the constraint on f_1 , when optimizing f_2 , with the relaxation of f_1 's constraints resulting in a slightly different distribution of Pareto solutions, particularly focusing on regions with higher f_1 and lower f_2 . Using tighter McCormick envelopes could potentially improve the HV, offering a more accurate representation of the Pareto front.

Step Size	Pareto Points	Runtime (Q)	Runtime (M)	HV (Q)	HV (M)
0.2	6	17.33	4.51	2.43	2.43
0.1	11	30.98	10.14	2.58	2.55
0.05	21	55.30	15.97	2.66	2.59
0.025	41	139.10	32.77	2.69	2.62
0.0125	81	266.12	69.70	2.71	2.63

Table 30: Comparison of Hypervolume Indicator for ε -constraints using QuadCon vs. McCormick for minimizing f_2 and constraining f_1

4.5 Visualization of Pareto Frontiers:

Figure 8 compares the non-dominated solutions obtained using different methods: Adaptive Weighted Sum (AWS) with QuadCon, AWS with one-layer McCormick, ε -constraints with QuadCon, and ε -constraints with one-layer McCormick for $n = 6480$, with a 100-second time cap on total runtime. The runtime includes overhead to prevent bias toward McCormick relaxation. Under this time cap, the results show: AWS with QuadCon yields 2 Pareto points, AWS with McCormick produces 6 points, ε -constraints with QuadCon gives 6 points, and ε -constraints with McCormick achieves 21 points. The Pareto solutions from each method are displayed, with most methods including the two extreme points of the Pareto front. Some points may overlap, making them less visible. Within each AWS and ε -constraints method, the QuadCon solutions are found in the McCormick results, but McCormick provides additional points within the same time limit. Figure 9 compares the Pareto points obtained for $n = 10800$ with a 300-second total runtime cap, using the same methods: Adaptive Weighted Sum (AWS) with QuadCon, AWS with one-layer McCormick, ε -constraints with QuadCon, and ε -constraints with one-layer McCormick. Under this setup, AWS with QuadCon yields 2 Pareto points, AWS with McCormick provides 6 points, ε -constraints with QuadCon results in 3 points, and ε -constraints with McCormick generates 21 points. The solutions shown in the figure highlight the performance of each method. As in the previous analysis, the two extreme points are included in most methods, and within each AWS and ε -constraints approach, the QuadCon solutions are found in the McCormick results, which offer additional points. Overall, Figures 8 and 9 demonstrate that McCormick relaxation facilitates a more thorough exploration of the Pareto front, leading to a higher number of non-dominated solutions for a given computational budget.

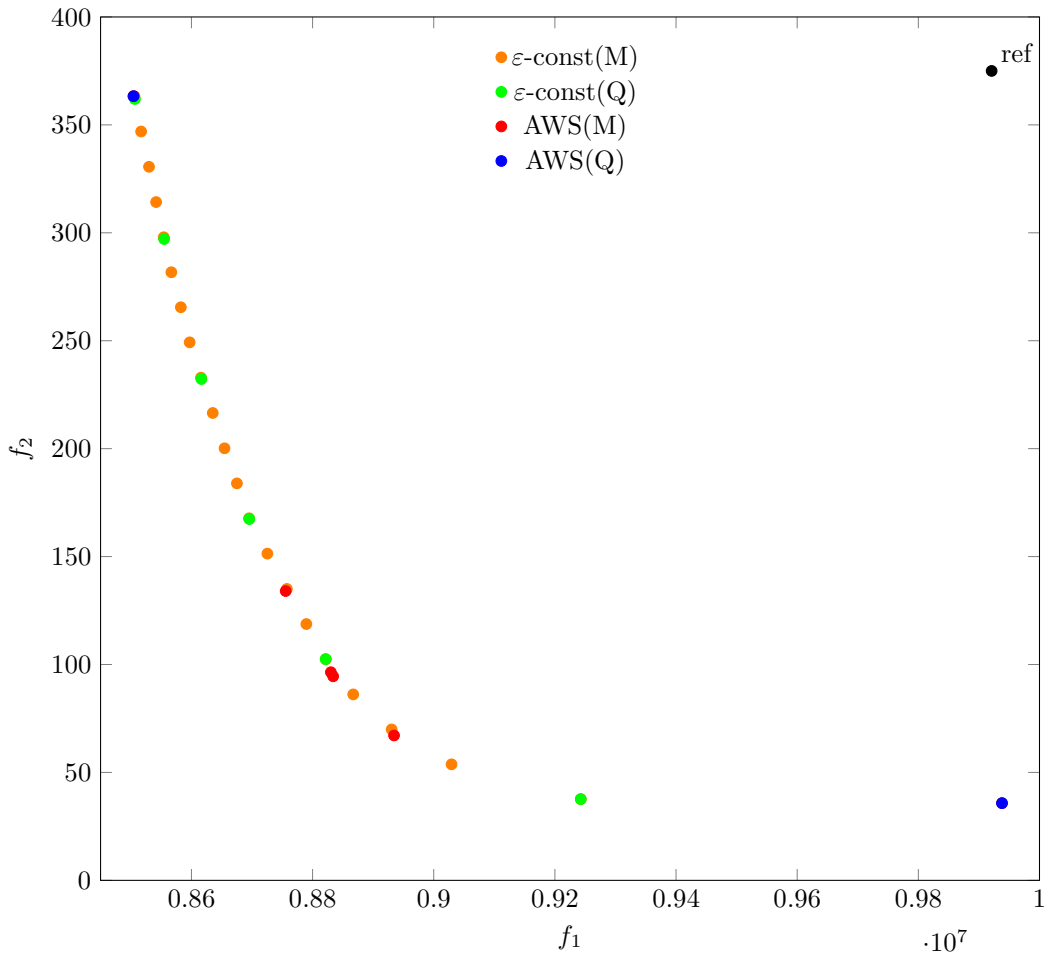


Figure 8: Pareto Points for Different Methods for $n = 6480$ with a time cap of 100 seconds

5 Conclusion

In conclusion, this work has focused on improving the efficiency of solving the Multiobjective Unit Commitment (MOUC) problem, when tackled through integer programming approaches. We investigated the use of adaptive weighted methods and epsilon constraints for calculating Pareto frontiers, highlighting their advantages over uniform weights, despite the added complexity of quadratic constraints. To address this, we introduced McCormick relaxations to approximate the problem with linear constraints, leading to significant improvements in computational performance on a real-world case study. The results showed only a minimal trade-off in solution quality compared to the standard Gurobi solver applied to the original formulation. Based on these promising results, we propose further theoretical analysis of the McCormick-based algorithm and its potential extension to other application domains beyond unit commitment. While this study did not compare with genetic algorithms, future work could explore integrating mathematical programming with evolutionary methods to further enhance the solution process for such problems.

Acknowledgment

The research was funded partly by the Deutsche Forschungsgemeinschaft (DFG, German Research Foundation) under Germany's Excellence Strategy — The Berlin Mathematics Research Center MATH+ (EXC-2046/1, project ID:390685689). The authors would additionally like to thank Prof. Falk Hante (Humboldt Universitaet zu Berlin) for insightful comments that helped with the technical aspects of this work.

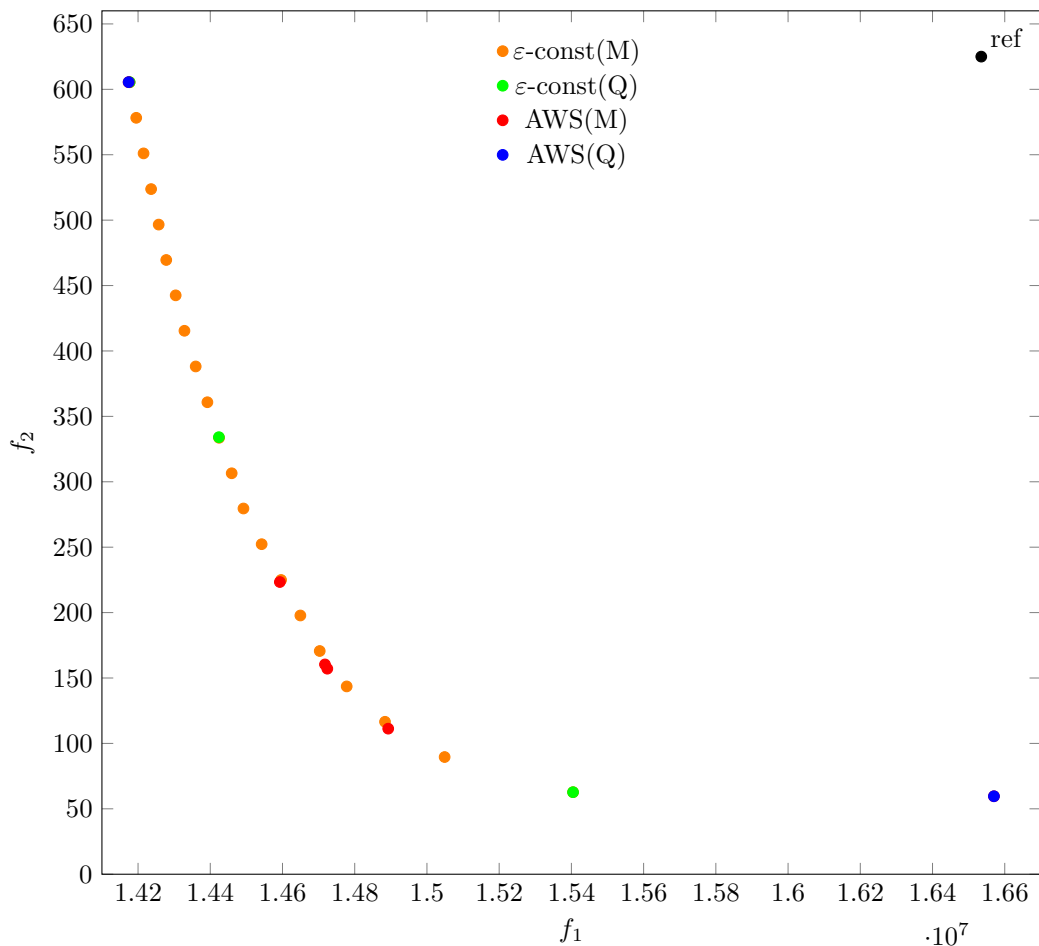


Figure 9: Pareto Points for Different Methods for $n = 10800$ with a time cap of 300 seconds

References

- [1] F. ANTONIO AND C. GENTILE, *Solving non-linear single-unit commitment problems with ramping constraints*, Operations Research, 54 (2006), pp. 767–775.
- [2] C. AUDET, J. BIGEON, D. CARTIER, S. LE DIGABEL, AND L. SALOMON, *Performance indicators in multiobjective optimization*, Tech. Rep. G-2018-90, Les cahiers du GERAD, 2018.
- [3] D. BERTSIMAS, E. LITVINOV, X. SUN, J. ZHAO, AND T. ZHENG, *Adaptive robust optimization for the security constrained unit commitment problem*, Power Systems, IEEE Transactions on, 28 (2013), pp. 52–63.
- [4] N. BEUME, G. RUDOLPH, ET AL., *Faster s-metric calculation by considering dominated hypervolume as klee’s measure problem.*, Universitätsbibliothek Dortmund, 2006.
- [5] A. BOMPADRE AND A. MITSOS, *Convergence rate of mccormick relaxations*, Journal of Global Optimization, 52 (2012), pp. 1–28.
- [6] E. A. BOYD, *Solving integer programs with fenchel cutting planes and preprocessing*, Neural Parallel & Scientific Comp., 1 (1993), pp. 453–466.
- [7] J. BRANKE, *Multiobjective optimization: Interactive and evolutionary approaches*, vol. 5252, Springer Science & Business Media, 2008.
- [8] C. C. CARØE AND R. SCHULTZ, *A two-stage stochastic program for unit commitment under uncertainty in a hydro-thermal power system*, in PREPRINT SC 98-11, KONRAD-ZUSE-ZENTRUM FÜR INFORMATIONSTECHNIK, 1998, pp. 98–13.
- [9] P. CASTRO, *Tightening piecewise mccormick relaxations for bilinear problems*, Computers & Chemical Engineering, 72 (2014).

- [10] I. DAS AND J. E. DENNIS, *A closer look at drawbacks of minimizing weighted sums of objectives for pareto set generation in multicriteria optimization problems*, Structural optimization, 14 (1997), pp. 63–69.
- [11] K. DEB, *Multi-objective optimization using evolutionary algorithms*, vol. 16, John Wiley & Sons, 2001.
- [12] D. DENTCHEVA, R. GOLLMER, A. MÖLLER, W. RÖMISCH, AND R. SCHULTZ, *Solving the unit commitment problem in power generation by primal and dual methods*, in Progress in Industrial Mathematics at ECMI 96, Springer, 1997, pp. 332–339.
- [13] S. DEY AND P. U. I. ENGINEERING, *Strong Cutting Planes for Unstructured Mixed Integer Programs Using Multiple Constraints*, Purdue University, 2007.
- [14] J. DOMBROWSKI, *Mccormick envelopes*, 2015.
- [15] S. FELTENMARK, K. C. KIWIEL, AND P. OLOV LINDBERG, *Solving unit commitment problems in power production planning*, in in: Operations Research Proceedings 1996 (U. Zimmermann et al. Eds, Springer-Verlag, 1996, pp. 236–241.
- [16] A. FRANGIONI, F. FURINI, AND C. GENTILE, *Approximated perspective relaxations: a project and lift approach*, Computational Optimization and Applications, 63 (2016), pp. 705–735.
- [17] A. FRANGIONI, C. GENTILE, AND F. LACALANDRA, *Solving unit commitment problems with general ramp constraints*, International Journal of Electrical Power & Energy Systems, (2008), pp. 313–326.
- [18] A. FRANGIONI, C. GENTILE, AND F. LACALANDRA, *Solving unit commitment problems with general ramp constraints*, International Journal of Electrical Power & Energy Systems, 30 (2008), pp. 316–326.
- [19] ———, *Tighter approximated milp formulations for unit commitment problems*, IEEE Transactions on Power Systems, 24 (2008), pp. 105–113.
- [20] ———, *Sequential lagrangian-milp approaches for unit commitment problems*, International Journal of Electrical Power & Energy Systems, 33 (2011), pp. 585–593.
- [21] M. FURUKAKOI, O. B. ADEWUYI, H. MATAYOSHI, A. M. HOWLADER, AND T. SENJYU, *Multi objective unit commitment with voltage stability and pv uncertainty*, Applied Energy, 228 (2018), pp. 618–623.
- [22] B. GJORGIEV, D. KANČEV, M. ČEPIN, AND A. VOLKANOVSKI, *Multi-objective unit commitment with introduction of a methodology for probabilistic assessment of generating capacities availability*, Engineering Applications of Artificial Intelligence, 37 (2015), pp. 236–249.
- [23] J. GOEZ, J. LUEDKE, AND D. RAJAN, *Stochastic unit commitment problem*, IBM Research Report RC24713 (W0812-119), (2008).
- [24] R. GOLLMER, M. P. NOWAK, W. RÖMISCH, AND R. SCHULTZ, *Unit commitment in power generation—a basic model and some extensions*, Annals of Operations Research, 96 (2000), pp. 167–189.
- [25] R. E. GOMORY, *An algorithm for the mixed integer problem*, tech. rep., RAND Corporation, 1960.
- [26] Y. HAIMES, *On a bicriterion formulation of the problems of integrated system identification and system optimization*, IEEE transactions on systems, man, and cybernetics, (1971), pp. 296–297.
- [27] B. F. HOBBS, M. H. ROTHKOPF, R. P. O’NEILL, AND H.-P. CHAO, *The next generation of electric power unit commitment models*, vol. 36, Springer Science & Business Media, 2006.
- [28] A. ŞIMA UYAR AND B. TÜRKAY, *Evolutionary algorithms for the unit commitment problem*, Turkish Journal of Electrical Engineering & Computer Sciences, 16 (2008).
- [29] A. KANNAN, A. R. CHOUDHURY, V. SAXENA, S. M. RAJE, P. RAM, A. VERMA, AND Y. SABHARWAL, *Hyperaspo: Fusion of model and hyper parameter optimization for multi-objective machine learning*, Proceedings of the IEEE International Conference on Big Data, (2021).
- [30] I. Y. KIM AND O. L. DE WECK, *Adaptive weighted-sum method for bi-objective optimization: Pareto front generation*, Structural and multidisciplinary optimization, 29 (2005), pp. 149–158.
- [31] I. Y. KIM AND O. L. DE WECK, *Adaptive weighted sum method for multiobjective optimization: a new method for pareto front generation*, Structural and Multidisciplinary Optimization, 31 (2006), pp. 105–116.
- [32] A. H. LAND AND A. G. DOIG, *An automatic method of solving discrete programming problems*, Econometrica, 28 (1960), pp. pp. 497–520.
- [33] E. K. LEE AND J. E. MITCHELL, *Integer programming: Branch and bound methods*, 2001.

- [34] Y. LI, H. LI, B. WANG, M. ZHOU, AND M. JIN, *Multi-objective unit commitment optimization with ultra-low emissions under stochastic and fuzzy uncertainties*, International Journal of Machine Learning and Cybernetics, 12 (2021).
- [35] G. MAVROTAS, *Effective implementation of the epsilon-constraint method in multi-objective mathematical programming problems*, Applied Mathematics and Computation, 213 (2009), pp. 455–465.
- [36] K. MIETTINEN, *Nonlinear multiobjective optimization*, vol. 12, Springer Science & Business Media, 1999.
- [37] J. E. MITCHELL, *Integer programming: Branch-and-cut algorithms*, 2001.
- [38] C. MURILLO-SANCHEZ AND R. THOMAS, *Thermal unit commitment with nonlinear power flow constraints*, in Power Engineering Society 1999 Winter Meeting, IEEE, vol. 1, 1999, pp. 484–489 vol.1.
- [39] R. O’NEILL, K. HEDMAN, E. KRALL, A. PAPAVALIOU, AND S. OREN, *Economic analysis of the n-1 reliable unit commitment and transmission switching problem using duality concepts*, Energy Systems, 1 (2010), pp. 165–195.
- [40] R. P. O’NEILL, A. CASTILLO, AND M. CAIN, *The iv formulation and linear approximations of the ac optimal power flow problem*, tech. rep., FERC, 2012.
- [41] ———, *A computational study of linear approximations to the convex constraints in the iterative linear iv-acopf formulation*, tech. rep., FERC, 2013.
- [42] A. PAPAVALIOU, S. OREN, AND R. O’NEILL, *Reserve requirements for wind power integration: A scenario-based stochastic programming framework*, Power Systems, IEEE Transactions on, 26 (2011), pp. 2197–2206.
- [43] C. PIKE-BURKE, *Multi-objective optimization*, Report accessible through www. researchgate. net, (2019).
- [44] J. SCOTT, M. STUBER, AND P. BARTON, *Generalized mccormick relaxations*, J. Global Optimization, 51 (2011), pp. 569–606.
- [45] T. SHIINA AND J. R. BIRGE, *Stochastic unit commitment problem*, International Transactions in Operational Research, 11 (2004), pp. 19–32.
- [46] A. SHUKLA AND S. SINGH, *Multi-objective unit commitment with renewable energy using gsa algorithm*, INAE Letters, 1 (2016).
- [47] A. TSOUKALAS AND A. MITSOS, *Multivariate mccormick relaxations*, Journal of Global Optimization, 59 (2014), pp. 633–662.
- [48] B. WANG, S. WANG, X. ZHOU, AND J. WATADA, *Multi-objective unit commitment with wind penetration and emission concerns under stochastic and fuzzy uncertainties*, Energy, 111 (2016), pp. 18–31.
- [49] S. J. WANG, S. M. SHAHIDEPOUR, D. KIRSCHEN, S. MOKHTARI, AND G. IRISARRI, *Short-term generation scheduling with transmission and environmental constraints using an augmented lagrangian relaxation*, Power Systems, IEEE Transactions on, 10 (1995), pp. 1294–1301.
- [50] L. WHILE, L. BRADSTREET, AND L. BARONE, *A fast way of calculating exact hypervolumes*, IEEE Trans. on Evolutionary Computation, 16 (2012), pp. 86–95.
- [51] D. YANG, X. ZHOU, Z. YANG, Y. GUO, AND Q. NIU, *Low carbon multi-objective unit commitment integrating renewable generations*, IEEE Access, 8 (2020), pp. 207768–207778.
- [52] S. ZHAI, Z. WANG, J. CAO, AND G. HE, *A new multi-objective unit commitment model solved by decomposition-coordination*, Applied Sciences, 9 (2019).
- [53] R. D. ZIMMERMAN, C. E. MURILLO-SÁNCHEZ, AND R. J. THOMAS, *Matpower: Steady-state operations, planning, and analysis tools for power systems research and education*, IEEE Transactions on Power Systems, 26 (2011), pp. 12–19.

This figure "image.png" is available in "png" format from:

<http://arxiv.org/ps/2501.07128v1>